CYPRUS UNIVERSITY OF TECHNOLOGY

DEPARTMENT OF CIVIL ENGINEERING AND GEOMATICS

Postgraduate Thesis

EFFECTS OF AGEING AND CORROSION OF REINFORCEMENT ON THE SEISMIC RESPONSE OF RC BUILDINGS

Eleni Mina

Limassol, September 2016

CYPRUS UNIVERSITY OF TECHNOLOGY

FACULTY OF ENGINEERING AND TECHNOLOGY

DEPARTMENT OF CIVIL ENGINEERING AND GEOMATICS

EFFECTS OF AGEING AND CORROSION OF REINFORCEMENT ON THE SEISMIC RESPONSE OF RC BUILDINGS

by

Eleni Mina

Limassol, September 2016

Approval form

Postgraduate Thesis

Effects of ageing and corrosion of reinforcement on the seismic response of RC buildings

Presented by

Eleni Mina

Dissertation Supervisor: Professor Christis Chrysostomou

Signature _____

Committee member:

Signature _____

Committee member:

Signature _____

Cyprus University of Technology

Limassol, September 2016

Intellectual rights

The approval of the thesis from the Department of Civil Engineering and Geomatics of the Cyprus University of Technology does not necessarily imply acceptance of the opinions of the author, on behalf of the Department.

I would like to thank my advisor Professor Christis Chrysostomou of the Department of Civil Engineering and Geomatics. He consistently allowed this paper to be my own work, but steered me in the right direction whenever he thought I needed it.

This work would not have been possible without the guidance of my tutor Professor Nicholas Kyriakides. His door was always open whenever I ran into a trouble spot or had a question about my research or writing, and for that I owe him my gratitude.

ΠΕΡΙΛΗΨΗ

Η σεισμική δραστηριότητα σε μια περιοχή μπορεί να προκαλέσει σημαντικά προβλήματα στο δομημένο περιβάλλον, πολύ περισσότερο δε στην περίπτωσει όπου τα κτήρια είναι μεγάλης ηλικίας και έχουν υποστεί φθορά. Η πιο συνήθης περίπτωση φθοράς κτιρίων από οπλισμένο σκυρόδεμα είναι η οξείδωση του οπλισμού. Επιπλέον, οι μηχανισμοί που προκαλούν την έναρξη της αποπαθητικοποίησης του χάλυβα όπως η ενανθράκωση καθώς επίσης και η διείσδυση χλωριόντων έχουν μελετηθεί επισταμένα κατά τα προηγούμενα χρόνια. Αυτή η μελέτη, στοχεύει στο να αναδείξει παράγοντες οι οποίοι επηρεάζουν τη μείωση της αντοχής των μελών κτιρίων από οπλισμένο σκυρόδεμα. Η μελέτη παρουσιάζει πως η μείωση της διαμέτρου του χάλυβα μετά από την οξείδωση επηρεάζει τη συμπεριφορά του κτιρίου όταν υποβληθεί σε σεισμικά φορτία, καθώς επίσης την μέγιστη παραμόρφωση του χάλυβα για τέσσερις χρονικές περιόδους. Επίσης επισημαίνει τις επιδράσεις της οξείδωσεις, εξηγώντας σε λεπτομέρεια τις συνέπειες της μείωσης της αντοχής. Επιπλέον, η μελέτη προσπαθεί να εξηγήσει την επίδραση του οξειδωμένου οπλισμού στη σεισμική συμπεριφορά κτιρίων οπλισμένου σκυροδέματος κατά τη διάρκεια του χρόνου, χρησιμοποιώντας δύο μη-γραμμικές μεθόδους ανάλυσης, τη στατική και την ανάλυση χρονοϊστορίας.

ABSTRACT

The presence of seismic activity in an area may cause severe problems to the building stock, especially in the case that the latter is old and has undergone some deterioration. The common case of deterioration of concrete structures is the corrosion of the reinforcement. Additionally, the mechanisms of initiation that usually lead to steel depassivation like the carbonation of concrete as well as the penetration of chloride ions have been studied thoroughly over the past years. This study, aims at highlighting factors that affect the decrease in the strength of the members of a reinforced concrete structure. The study presents how the decrease of the steel diameter after corrosion is affecting the structure response under various seismic loadings and also the ultimate steel deformation for four time intervals. It also highlights the effects of corrosion, explaining in detail the consequences from the decrease in strength. In addition to the above, this study attempts to explain the impact that corroded reinforcement has on the seismic response of concrete buildings over time, using two nonlinear methods of analysis, the pushover and the time history one.

TABLE OF CONTENTS

TABLE OF TABLES

TABLE OF FIGURES

ABBRIVIATIONS

ε_c: Compressive strain in the concrete

ε_{c2}: Compressive strain in the concrete at the peak stress

ε_{cu2}: Ultimate compressive strain in the concrete

ε_y: Strain at yield point

ε_s: Compressive strain in the reinforcement

E_s: Design value of modulus of elasticity of reinforcing steel

A_s: Cross sectional area of reinforcement

f_c: Concrete compressive strength (MPa)

f_{ck}: Characteristic compressive strength of concrete

f_{yk}: Characteristic yield strength of reinforcement

h: Depth of cross section

b: Width of cross section

d': Depth to the compression reinforcement

N: Column axial force

α: Confinement effectiveness factor

ω, ω': Mechanical reinforcement ratio of tension and compression reinforcement

L_v: Shear span at member end

S_h: Shear links distance

b_o, h_o: Dimension of confined concrete core to the centerline of the hoop

b_i: Centerline spacing of longitudinal bars

ρ_{sx}: Ratio of transverse steel parallel to direction x of loading (Sh: stirrup spacing)

f_{yw}: Yield stress of transverse or confinement reinforcement

ρ_d: Steel ratio of diagonal reinforcement

KL1: Knowledge level 1

ρ_{tot}: Total longitudinal reinforcement ratio

ρ_w: Transverse reinforcement ratio

z: Length of internal lever arm

Introduction

The optimal performance of concrete is usually the most critical feature required for durability. Most structures have reported the problem of unsatisfactory toughness as well as strength during natural disasters like earthquakes (Coronelli et al., 2004). The above findings not only lead to economic impacts but also to environmental, industrial and social problems because of the risk of safety and reliability. The rates and types of degradation processes of concrete, as well as the reinforcement, usually define the rigidity or the resistance of the material being used and also reflect on the structural appearance of the structure. The deterioration of concrete, as well as steel in service, is considered to be the cause for loss of performance. This usually results due to various mechanical, chemical, physical or even biological processes. The major final result of the above mechanism is usually the formation of a crack. Cracking tends to occur whenever the tensile strain to which concrete is subjected to tends to exceed tensile strain capacity (Tuutti, K., 1982). The corrosion of steel reinforcement is considered as the most serious problem of reinforced concrete buildings.

The purpose of this study is to examine a seven-storey building model which follows old design codes and construction regulations, and investigate the effect of the corrosion of reinforcement at 0, 25, 50 and 75 years, based on mathematical models retrieved from Kombou 2015. This model has been developed in the software SAP2000 as a two-dimensional multi-storey frame building. The reduction of the steel area and the maximum steel deformation were calculated for the four periods.

On the basis of the above, the moment – curvature relationship was produced for the columns and beams of the building according to Eurocode 8 - Part 3. Then, these curves were introduced in the software model to describe the behaviour of plastic hinges that were placed at both the edges of every member. Following this, joint loads at each level were applied in order to perform the pushover analysis, and generate force – displacement curve of the building for each one of the time intervals mentioned above.

Examination of the force-displacement curves revealed the type of failure mechanism, whether it was shear or bending failure, for each member. For the time history analysis six different earthquakes were examined to obtain the failure acceleration for each one of the time intervals.

1 Corrosion

Corrosion can be defined to be the gradual destruction of materials especially metals by various chemical reactions with their surroundings. In other words, it can be described to be the disintegration of an engineering material into their constituent atoms due to the chemical reactions in their environment (Stewart, 2004, Stewart et al., 1998).

The corrosion of the reinforcing steel as well as other metals that are embedded is the major cause of concrete deterioration. When steel corrodes, the rust from the result occupies larger volumes of the steel. The above expansion leads to the creation of tensile stress in the concrete that can cause cracking, spalling as well as delamination. Corrosion with rusting of the reinforcement comprises various stages. In the first stage, aggressive elements like carbon dioxide and chloride ions that are present in the surrounding medium usually penetrate the concrete. This acts as the stage of initiation. The next stage is comprised of propagation that starts when the above aggressive element appears in rather large concentrations around the reinforcement. This stage corresponds to the growth of rust that leads to the breaking of the concrete cover. It is, therefore, important to understand the penetration mechanisms of the aggressive agents through the concrete as well as the conditions of depassivation of the reinforcement.

1.1 The course of corrosion

The chloride is produced by the building being exposed in an airborne chloride environment. Oxidation of the reinforcing bars is an electrochemical phenomenon that takes place in several stages through complex mechanisms. It occurs when iron is constantly surrounded by moisture, which penetrates into the concrete surface through the cracks. The result of the oxidation is the iron loss due to the disruption of the crystalline structure and uniform peel oxidized portions of the entire surface. In the final phase, detachment of concrete parts and display of reinforcement bars takes place. Corrosion can, therefore, be classified to be a process that is complex and has the capability of affecting the RC structures.

1.2 The effects of corrosion

Corrosion has various effects on structures. The major effect of corrosion is that it severely reduces the strength as well as the life of the structures. Consequently in humid conditions pollutants from the atmosphere percolate via the concrete cover. This usually causes corrosion of the steel during the construction. After this process of the initiation of corrosion on the reinforcing steel, the products of corrosion usually expand and occupy a larger volume approximately 10 times greater than that of the steel used. This results in the formation of cracks and finally leads to the failure of the structural members.

Structural steel accounts for the major portions of the metals that are used in building construction around the world. Fortunately, the steel is usually located within the construction and is always shielded from the outdoor environment by the exterior concrete finish. In cases where the structural steel is exposed to water from rain or the condensation of water vapor, corrosion results and it endangers the structure making it weak. Additionally, corrosion is considered as a major environmental degradation mechanism of the RC structures loss of steel reinforcement.

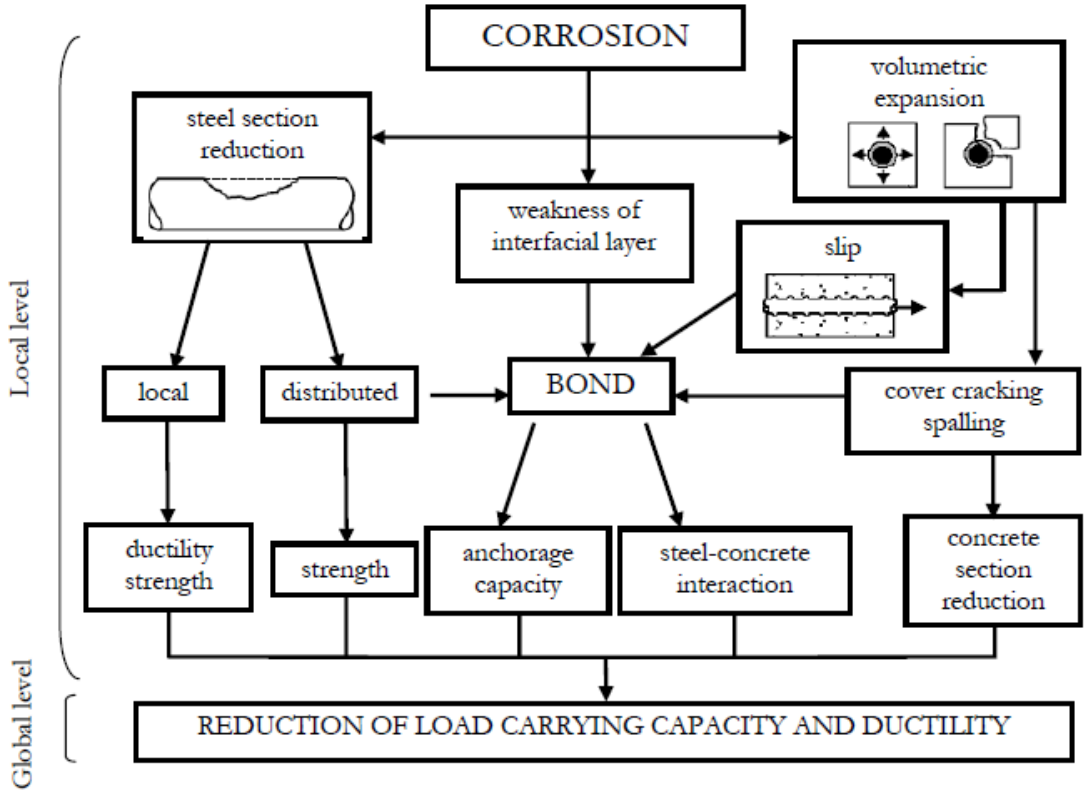

Figure 1: Corrosion effects on the structural performance (Simioni, 2009)

The deterioration of the concrete structures as a result of the harsh environmental conditions usually leads to the performance degradation of the RC structures. This also leads to the premature deterioration of the structures immediately before completing the expected life service which is now a basic concern for all the civil engineers as well as researchers.

Deterioration rate of materials usually depends on the exposure conditions as well as the extent of maintenance. Findings from various researches have proved that corrosion is the major cause of deterioration of most of the concrete structures.

1.3 Initiation of corrosion

From FIB-CEB Task Group 5.6 (2006) the initiation of corrosion can be expressed as follows:

$$T_{ini} = \left(\frac{\alpha^2}{4.ke.kt.D_{RCM,0}.(t_0)^n} . \left(erf^{-1}\left(1 - \frac{C_{crit}}{C_s}\right)\right)\right)^{\left(\frac{1}{1-n}\right)} \quad \text{(Years)} \qquad (1)$$

Where, α = concrete cover depth (mm); ke = the environmental function; kt=transfer variable 0.832; $D_{RCM,0}$ =the chloride migration coefficient (m^2/s); t_0 = reference point of time (years); n = aging exponent; erf^{-1}= Gaussian error function; C_{crit} =critical chloride content (wt/cement %); C_s = equilibrium chloride concentration at concrete surface (wt/cement %).

1.4 Steel area loss and degree of corrosion

The continuous penetration of the chloride elements in the concrete is causing the passive film of the reinforcement to dissolve; thereafter corrosion starts its course and the loss of its cross sectional area counting on the passage of time can be expressed as follows (Ghosh and Padgett, 2010):

$$A(t) = \begin{cases} n.Di^2\frac{\pi}{4} & when\ t \le Tini \\ \max\left[n.(D.(t))^2.\frac{\pi}{4}, 0\right] & when\ t \ge Tini \end{cases} \qquad (2)$$

Where, n = number of reinforcement bars; Di= initial diameter of steel; t= elapsed time (years); D(t) = reinforcement diameter at the end of (t-Tini) years which is formulated as:

$$D(t) = Di - i_{corr} . \kappa . (t - T_{ini}) \qquad (3)$$

Where, i_{corr} = rate of corrosion (mA/cm^2); κ= corrosion penetration (μm/year, uniform corrosion penetration for generalized corrosion).

2 Factors affecting the strength of members

Various factors affect the strength of reinforced concrete members. The following include critical exposure conditions as well as deterioration mechanisms in concrete. Additionally, concrete can easily withstand the effects when designed properly.

Moreover, concrete usually expands slightly due to the temperature increase and contracts once the temperatures fall. This change usually leads to cracking of the concrete members leading to corrosion of the reinforcement. Shrinkage potential of the concrete mixtures used as building materials is usually perhaps the most critical considerations for the concrete used to construct floors as well as the base of most structures. The rates and types of degradation processes of concrete, as well as the reinforcement, usually define the resistance or the rigidity of materials being used. This, therefore, reflects the serviceability, the safety and the structural appearance, for instance, it tends to determine the performance of that structure.

2.1 Corrosion of reinforcement

One important parameter in the nonlinear analyses of reinforced concrete structures is tension stiffening after the crack has occurred. It is clear that the average tensile strength of reinforced concrete numbers usually does not reduce abruptly to the value, zero after the tensile crack has occurred. The excessive tensile stress usually results in cracking of the reinforced concrete member (Neville, 1995). Consequently, all the tensile forces that are applied to the crack faces tend to pass through the steel reinforcement. This usually results in the transfer of the tensile forces that result from the steel reinforcement to the concrete by the bond stresses located between steel bars as well as the concrete that surrounds. This results in a tension stiffening phenomenon on the structures.

2.2 The deterioration of the concrete cover

Concrete covers that surround the reinforcement can experience deterioration by the environment because of different reasons. The first reason is due to physical causes like freezing, mechanical causes like cracks on the concrete due to excessive loadings and chemical causes for instance due to bodies like ions contained within the environment. The reinforced concrete structures are usually in contact with the atmosphere for example water or in contact with the ground. The above environments are sometimes polluted and tend to

contain agents that can enter the concrete causing it to modify its characteristics. The common aggressive agents are known to be pure water, carbon dioxide in the atmospheres as well as chloride ions dissolved in water.

2.3 Concrete surface cracks

The sort and measure of the breaks on the surface of concrete, for the most part, have a basic impact on the sturdiness of the concrete. Splits that are caused by the shrinkage or the expansion may once in a while contribute essentially to the erosion of fortification. This is especially true when they run parallel to the strengthening bars or when they are nearer to the concrete surface.

In any case, flexural splits tend not to be an issue, since they diminish in width from the most extreme at the surface while get to be smaller at the levels of the steel utilised for reinforcing. The penetration of the corrosion inducing agents like the chloride ions as well as the carbon dioxide that is increased at the crack sites further increases the levels of corrosion. This will widen and expand the cracks on the concrete to expose more steel. The cracks increase the rate of corrosion because they expose more steel to the atmosphere. (Rodriquez, and Andrade, 2001)

Corrosion simply reduces the toughness of structures. During the process of corrosion, the steel bars are corroded hence become weak. This reduces the total support given to the concrete. After continuous corrosion and corroding of the steel, the concrete becomes heavier making the whole structure to loose balance. This may lead to the collapse of buildings or bridges.

3 Construction materials

The excessive tensile stress usually results in cracking of the reinforced concrete member. This usually results in the transfer of the tensile forces from the steel reinforcement to the concrete by the bond stresses located between the steel bar and the surrounding concrete. This lack of toughness usually results in massive as well as increased costs due to increased maintenance, consequential building damages and extensive replacements.

3.1 Ageing of materials

It can be defined as the gradual process where various properties of material, system or structure change over time or with use. This can be due to biological, physical or chemical agents like corrosion, weathering and obsolescence. It is, therefore, the change in the physical, mechanical and other chemical properties of the metal as well as their alloys.

Building materials, components, as well as assemblies, have to fulfil their functional demand during the lifetime of a building. The materials, therefore, must possess satisfactory toughness on the properties (Hooton, Stanish and Thomas, 2001). However, the resulting experience is unfortunate that most materials often do not satisfy the requirements after a relatively short time of use. This lack of toughness usually results in massive as well as increased costs due to increased maintenance, consequential building damages and extensive replacements. The ageing of building products usually leads to failure of the building materials. The failure, in turn, may also result in increased health hazards and the impacts of the hazards when they occur.

Natural disasters that cannot be controlled like earthquakes could have negative impacts on aged materials, which is quite dangerous. Some of the natural disasters tend to break or collapse structures causing damages to the individuals. It is, therefore, important to explore and employ the use of materials that have higher toughness during construction.

3.1.1 Factors of ageing

Ageing does occur in various ways. Firstly, the natural outdoor climate ageing process, which usually takes longer to occur. This can be as a result of natural causes like the atmosphere, the rain or the type of materials used. The process takes longer time depending on the economy.

The quality of the structures constructed depends on the economy and the prices of materials employed. Durable materials are usually expensive making the real estate owners opt for cheaper materials that are prone to ageing.
Building structures are always subjected to large as well as changing climatic strains. These climatic strains cause the ageing of the building materials. Examples of the climatic strains due to exposure climate factors include the wind, physical strains, earthquakes, oxygen, time, pollutions, erosion etc. However, other parameters participate such as the water cement ratio for the variety of concrete types, the cement quality etc. (Simioni, 2009)

3.1.2 Ageing of concrete

Additionally, concrete usually expands slightly due to the temperature increase and contracts once the temperatures fall. With some of the ageing structures, heat cannot be dissipated. This change usually leads to cracking of the concrete members resulting in the collapse of the structures. Admittedly, the shrinkage potential of the concrete mixtures used as building materials is usually perhaps the most critical considerations for the concrete used to construct floors and the ground of most structures. Concrete shrinkage due to the loss of volume tends to lead to cracking when restraints like the base friction occur.

3.2 Water to cement ratio

The properties of the concrete are significantly influenced by the water to cement ratio. This ratio is calculated by the weights of the two materials, water and cement. Those two ingredients are responsible for the binding of the mix, providing strength and durability to the concrete when cured. More specifically, in the area of Cyprus the ratio of 0.4-0.45 is used for the production of concrete mixes, which means 100kg of cement requires 40kg of water. The range of the ratio is sometimes at the client's preference.

Although more types of cement are produced, such as CEM II/B-L 32.5R, CEM II A-L 42.5R, CEM I 52.5N, CEM I 52.5N-SR5 and CEM II/A-L 42.5N (white), the most common types used are CEM II A-L 42.5R and CEM I 52.5N. More specifically, type CEM II A-L 42.5R is chosen more often because is the most cost effective.

The best way to think about the w/c ratio is to think that the more water added to the mix, the more strength loss the concrete has. Also it affects the porosity, tensile and flexural strengths of the material.

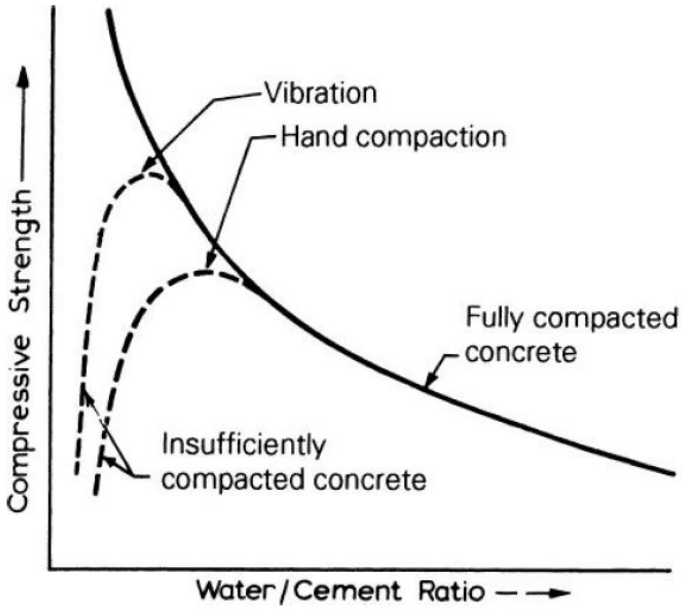

Figure 2: The relation between strength and water to cement ratio of concrete (Neville, 1995)

3.3 Surface treatment of the concrete

Amid the creation of the structural completions, the concrete surfaces are washed repeatedly. The above practice is highly suggested in situations where there exists the likelihood of forceful compound like acids or even salts that penetrate the cement. Washing, carving or mechanical concrete surface completion may now and then result in the loss of important bond rich glue that structures the surface of the concrete. This will diminish the carbonation resistance and also the profundity of the spread.

3.4 Nature of the concrete

The basic property of the concrete is typically the penetrability. In this way, the degree of porousness has a tendency to decide and additionally rate the dispersion of the chloride particles or carbon dioxide using the concrete. Porousness can be said to be a component of a mix of configuration, curing and additionally compaction.

3.5 Profundity of the spread on cement

The absence of the concrete spread for the support has been recognised to be the significant issue connected with most disappointments in the tall structures. In many overviews of right

around ninety-five structures in Sydney that reach in the range from 6 to 35 stories and matured 2 to around 18 years, the normal profundity of the concrete at sights where the spalling happened was appraised to be 5.40mm (Ramamoorthy et al., 2007). This demonstrates the profundity of the spread is a critical element in deciding the quality of the structure.

3.6 Concrete environment exposure

Reinforced concrete structures are exposed to the atmosphere and get in touch with parameters such as water or the ground. The environment is made out of operators that bring the erosion of the reinforcement. Some of these specialists incorporate oxygen, carbon dioxide, water and chloride particles. Structures that are normally situated to the seaside areas are thought to be in danger from erosion of support because of the entrance of the chloride particles coming from the ocean splash and salt loaded wireless transmissions.

The type, as well as the size of the cracks on the surface of the concrete, usually has a critical influence on its performance. Structures that are usually close to the coastal regions are considered to be at risk from corrosion of reinforcement due to the ingress of the chloride ions that occur from the sea spray as well as salt-laden airwaves. In cases where the structural steel is exposed to water from the rains or the condensation of water vapour, corrosion results and it endangers the structure making it weak. The deterioration of the concrete structures as a result of the harsh environmental conditions usually leads to the performance degradation of the RC structures.

On the mainland's, the vast majority of the consumption of the reinforcement have a tendency to happen due to procedures coming about because of carbonation. This procedure lessens the alkalinity of the encompassing cement. Like this, the procedure can happen in any given geographic area that encompasses the concrete.

4 Structural vulnerability

Earthquakes are vibrations that sometimes tend to cause shaking to the earth's surface which follows emissions of energy within the crust of the earth. The energy above is usually generated due to the sudden dislocation on the segments of crusts of the earth's surface. This usually occurs via volcanic eruptions or even due to manmade explosions. The dislocation from the crusts usually leads to the generation of destructive earthquakes. During the earthquake process, the crust tends to bend, leading to the rocks breaking. During the process of breaking, vibrations are released which are known as seismic waves. The waves have the ability to travel out from the earthquake sources along a surface as well as through the earth at differentiated velocity. These waves are the ones that cause the disasters on the surface of the earth (Choe et al., 2009).

4.1 Seismic vulnerability

Various experimental testing is adequate to determine the seismic performance of buildings. Additionally, it is not feasible to effectively determine the seismic performance of the stock of buildings located in places like cities experimentally by testing the representative model. The seismic performance of the structured stock located in the city can, therefore, be determined using techniques known as the risk assessments techniques (Angst, 2011). This seismic risk evaluation can, therefore, be defined as the combination of the seismic hazard as well as vulnerability. Moreover, the seismic hazard depends on upon the geology of the region under consideration. This gives a specific characteristic to the structure. Seismic vulnerability, on the other hand, depends on the materials of the structure (Simioni 2009), mechanical properties of the materials used during construction, details of the structural components, the details of connection, and the layout as well as the geometry of the structure. Different approaches can be applied regarding the assessments of the seismic vulnerability of the structure.

4.2 Observed vulnerability

The vulnerability methods of assessment of expert opinions are usually applicable to the areas that have experienced earthquakes over the past years. However, for the other areas, analytical strategies used for determining the seismic vulnerability are required. The analytical methods that employ simple models of the building are usually based on a small number of input

parameters. These parameters consequently have the advantage of analysing a larger number of buildings relatively in a short period or duration of time. Besides, the efficiency of the method usually increases when the input parameters that are required for the process of analysis of the building can effectively capture overall seismic behaviour of the structures.

In the present study, nonlinear time history analysis is used for stimulating the structure behaviour under severe earthquakes since it is considered to be more appropriate than other methods. The nonlinear dynamic analysis employs the combination of the record of ground motion using a detailed structural model (Vu, 2000). It has the capability of producing the results that have relatively low uncertainty.

During nonlinear dynamic analyses, detailed structural models that are subjected to the ground motion record usually produce estimates of the components of deformations for each degree of freedom. The nonlinear properties are also considered to be part of the time domain analysis. This is a rigorous approach and is therefore required by various building codes for buildings that have unusual configuration.

5 Pushover analysis

It is the common name of the procedures which use simplified nonlinear static analysis, to indicate the structural member yielding and failure modes. Therefore, is said to be a static nonlinear analysis method that involves the subjection of a structure to the gravity loading as well as monotonic displacement controlled load pattern (Mohammed et al., 2014). Moreover, increasing lateral forces can be applied to a structure until it becomes unstable and reaches a predetermined limit (Ramamoorthy, 2006).

The basic reason for performing a nonlinear pushover analysis to the frame was to examine the original column failure and failing point at different periods of time. The analysis was performed for 0, 25, 50, and 75years. The procedures of the analysis along with the results are presented in section 7.

5.1 Nonlinear push over analysis

For the nonlinear analysis, some of the components used have the ability to yield (Fotopoulou et al., 2012). Additionally, inelastic properties sometimes are required for the above components. The process of nonlinear analysis is more complicated than an elastic one. In the nonlinear analysis, there are also calculations of the inelastic deformations as well as the performance which is assessed by using both deformation and strength. These can continuously increase via elastic as well as inelastic behaviour until they reach an ultimate condition. Consequently, various limitations are currently in place. For instance, all the nonlinear properties that usually determine the possible structure damage as a result of the forces from the earthquakes are concentrated in nonlinear hinges (Porter et al., 2015).

5.2 Stages of pushover analysis

A critical limitation is that the users usually predetermine the nonlinear hinges which is the method used in this study. The stages of the analysis start with the definition of the nonlinear hinges within a structure. Then, there is a step of assigning the nonlinear properties to the hinges. Further, performing the structure analysis for the model just to determine a single mode is done. It is also important to identify the parameters of the nonlinear analysis before the start of the analysis. The next step involves the determination of the capacity curve and last but not least, the performance point stepwise.

6 Time History Analysis

Time history analysis provides a nonlinear or linear evaluation of the structural dynamic responses under loading that tends to vary to the time function specified. The analysis obtains the structure's response for each one of the time intervals and provides an evaluation of the seismic behavior of the building model.

The observation of the seismic behavior of the model with the time history analysis requires the use of accelerograms. The accelerograms had multiple peaks and were repeatedly forcing the structure to the nonlinear range. The seismic data were extracted by the following earthquakes used by Zinonos 2015.

Table 1: Seismic data used for the time history analysis

No	Earthquake Name	Date	PGA (g)	Location
1	Friuli	1976	0,248	Tolmezzo
2	Montenegro	1979	0,25	Hercegnovi
3	Kalamata	1986	0,239	Greece
4	Loma Prieta	1989	0,254	USA
5	Imperial Valley	1979	0,268	USA
6	Imperial Valley	1940	0,255	USA

6.1 Accelerograms used in the study

The accelerograms for the above earthquakes are presented as follows:

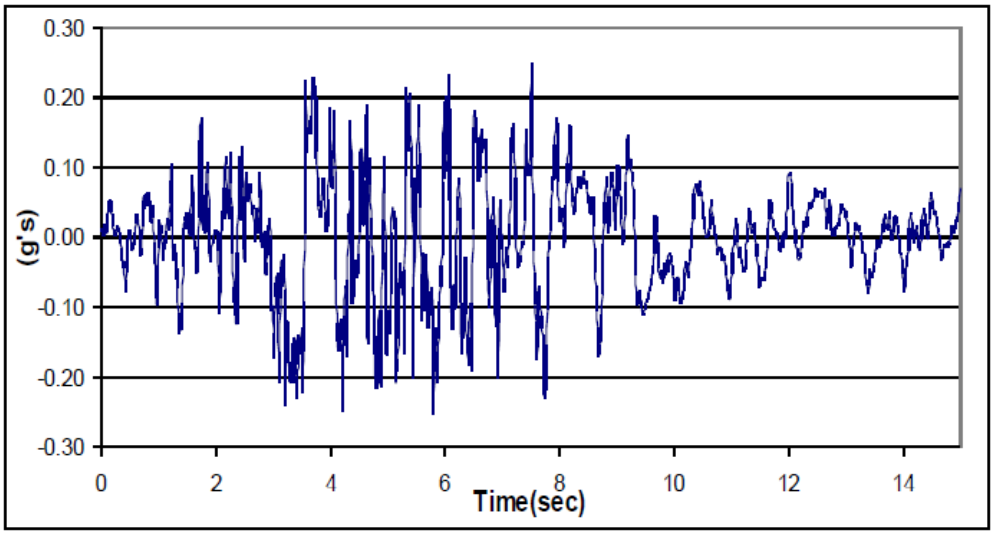

Figure 3: Seismic acceleration Friuli 1976, Tolmezzo Italy

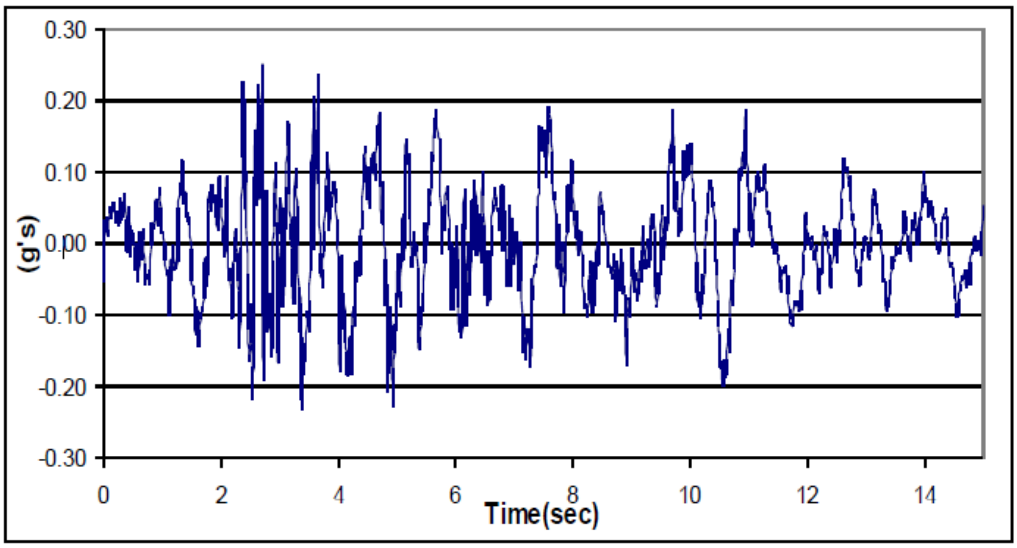

Figure 4: Seismic acceleration Montenegro 1979, Hercegnovi

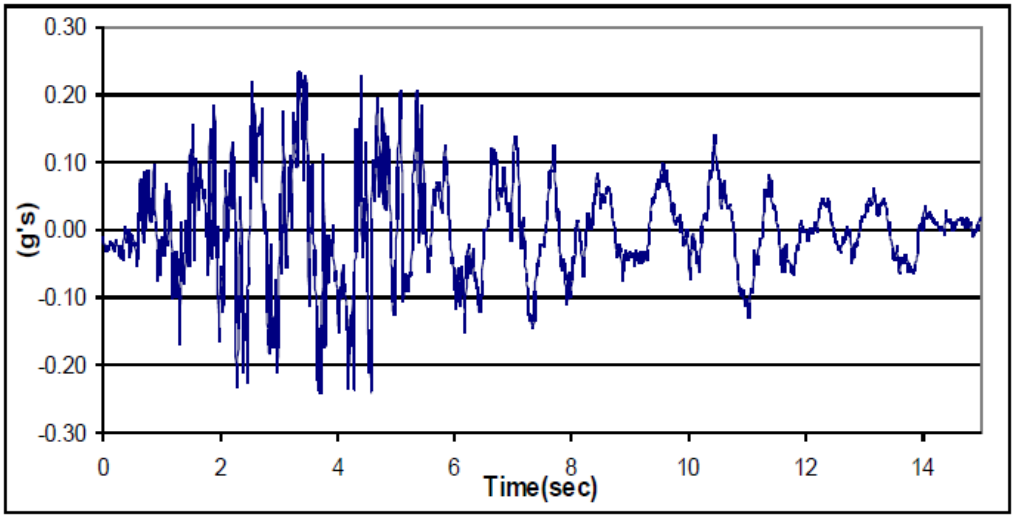

Figure 5: Seismic acceleration Kalamata 1986, Greece

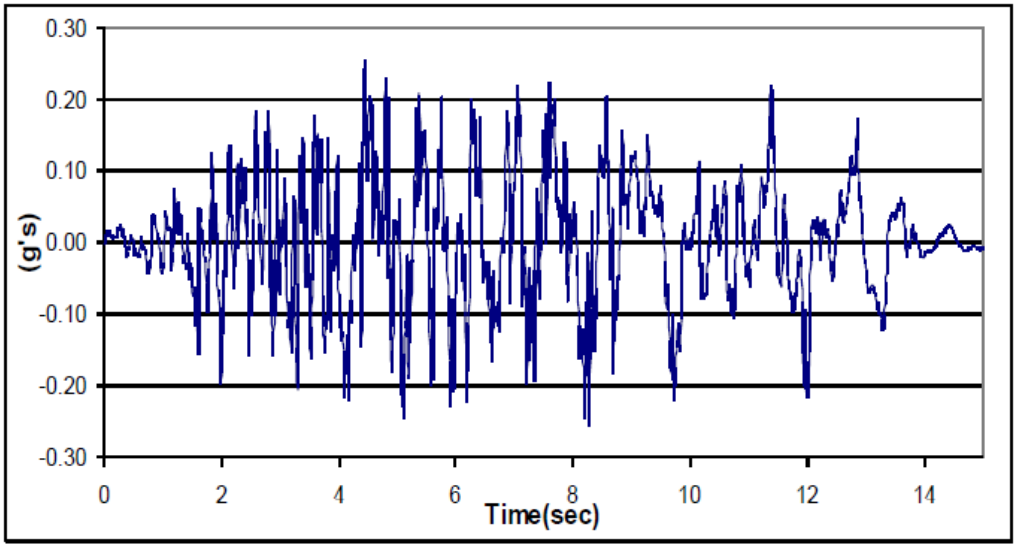

Figure 6: Seismic acceleration Loma Prieta 1989,Capitola USA

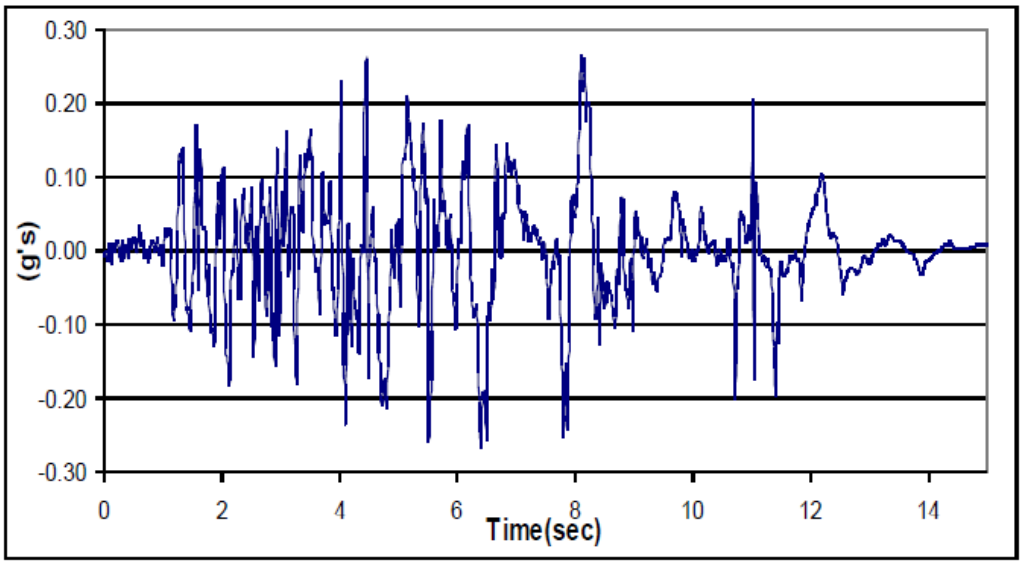

Figure 7: Seismic acceleration Imperial Valley 1979, Bonds Corner USA

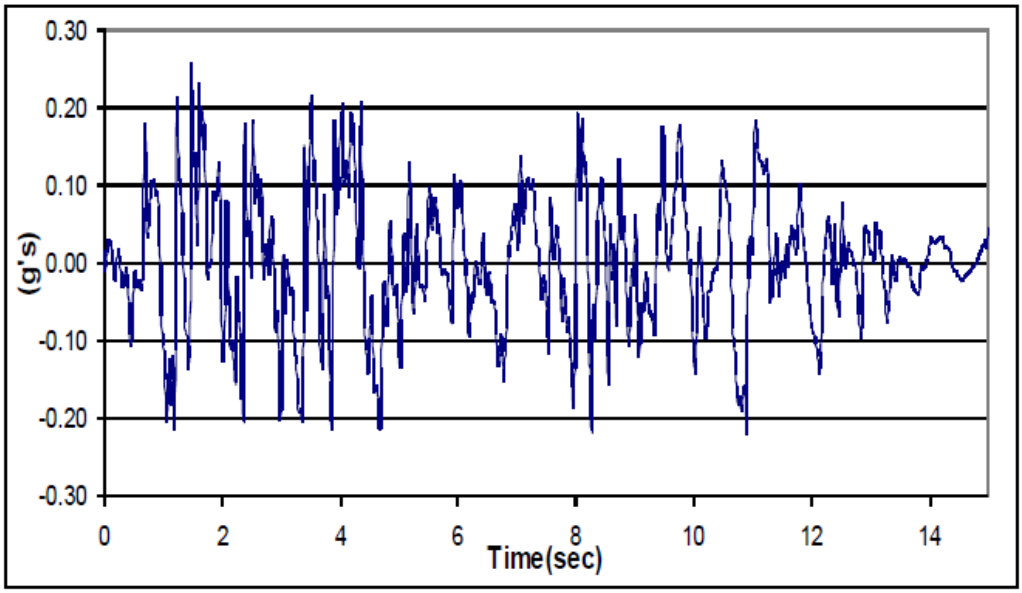

Figure 8: Seismic acceleration Imperial Valley 1940, El Centro Array #9 USA

7 Structural model

7.1 Building description

A 7-floor building model with 3m height each was tested in this study. It contained five frames of 5m each in the X-Direction and four frames of 5m each in the Z-Direction. Moreover, it was designed in a two dimensional form in SAP2000 software, considering a middle frame within which would give the worst case scenario of failure under specific loading.

7.2 Sections characteristics.

The columns were 425mmx425mm with a reinforcement of 12Y18 and 300mmx600mm beams with 8Y18. The shear links of Y8/20 were considered to be the same in all beams and columns and so was the concrete cover of 20mm. The slabs were considered to be 200mm in thickness. The analysis uses a characteristic strength of concrete C16/20 and 410 MPa for steel.

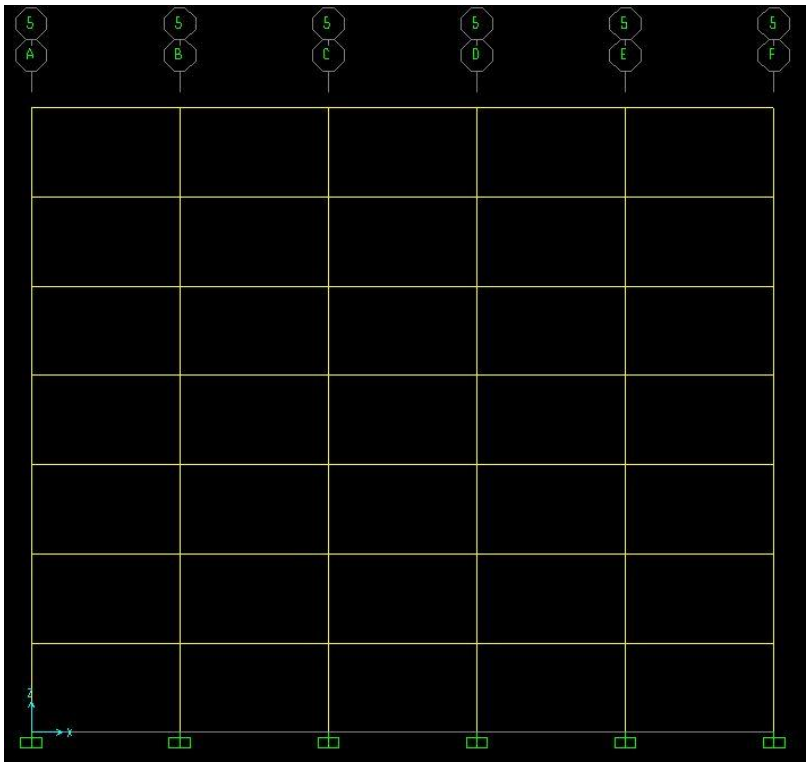

Figure 9: Model used for failure modes and seismic adequacy through time evaluation.

7.3 Corrosion Model

The corrosion model, as mentioned before, was used to calculate the initiation time of corrosion within the members of the reinforced concrete for the scenarios of 0, 25, 50 and 75 years. The figure below states the start time of corrosion after penetration of chlorides in the concrete, according to the methodology mentioned earlier in Section 3. As stated in Kombou 2015, the methodology of obtaining the steel area loss after corrosion effects was also used in this study.

Time period of initiation of corosion *(in years)*

$$T_{ini} = \left(\frac{a^2}{4 * k_t * k_e * D_{RCM,0} * (t_0)^n} * \left(erf^{-1} * \left(1 - \frac{C_{crit}}{C_s} \right) \right)^{-2} \right)^{\left(\frac{1}{1-n}\right)}$$

		Values from study
α :	*Cover depth (mm)*	20
k_t:	*Regression parameter*	1,25
k_e:	*Environmental function*	0,67
$D_{RCM,0}$:	*Rapid chloride migration coefficient (m^2/s)*	643,33
t_0:	*Time reference point (28/365)*	0,0767
n:	*Aging exponent*	0,362
C_s:	*CO_2 concentration @ surface (kg/m^3)*	1,41075
C_{crit}:	*Critical chloride content (water/cement)*	0,6
$erf^{-1}*(1-C_{crit}/C_s)$:	*Gaussian error function*	0,558
T_{ini}:	*Corrosion initiation time in years*	**1,91**

Figure 10: Automated excel spreadsheet for calculation of corrosion initiation.

The start time of corrosion was found to be 1.91 years based on the statistical data presented in the table below.

Table 2: Values on the basis of the Cypriot data in general.

Water/Cement ratio 0,45 - CEM II A-L 42,5 R.				
Parameter	**Mean**	**COV**	**Distribution**	**Reference**
cover a	20	0,4	*Lognormal*	Karapetrou et al [2013]
Ke	0,67	0,17	*Normal*	
Kt	1	constant value		FIB-CEB Task [2009]
$D_{RCM,0}$	389,47	0,2	*Normal*	Kombou [2015]
[mm2/yr]	*(8,9E-12+1,58E-11) / 2=*		*1,24E-11*	
n	0,362	0,677	*Beta*	Choe et al. (2009)
		a=0.0, b=0,98		
t_0	0,0767	–	*Constant*	FIB-CEB Task [2009]
Ccrit [wt/cement%]	0,6	0,25		
		a=0,2, b=2,0	*Beta*	
Cs[wt/cement%]	1,15425	0,2	*Normal*	Choe et al. (2009)
	(1,2825+1,026)/2=		*1,15425*	
i_{corr} $[mA/cm^2]$				Stewart [2004]
Low	0,1	0,25	*Normal*	
Medium	1			
High	10			

Furthermore, the loss of the main bar reinforcement, as well as shear links, due to corrosion appears in the figures below, for all four scenarios.

Reinforcement diameter at the end of ($t-T_{ini}$)

$D_{(t)}=D_i-i_{corr}*k*(t-T_{ini})$

		Values from study	
		Longitudinal bars	**Shear links**
D_i:	*initial steel diameter (mm)*	18	8
i_{corr}:	*rate of corrosion (mA/cm^2)*	10	10
k:	*corrosion penetration (μm/year)*	11,6	11,6
t:	*time (years)*	25	
T_{ini}:	*Corrosion initiation time in years*	1,91	1,91
$D_{(t)}$:	*reduced steel diameter(mm)*	**15,32**	**5,32**

Figure 11: Automated excel spreadsheet for the remaining steel diameter after 25years.

Reinforcement diameter at the end of ($t-T_{ini}$)

$D_{(t)}=D_i-i_{corr}*k*(t-T_{ini})$

		Values from study	
		Longitudinal bars	Shear links
D_i:	*initial steel diameter (mm)*	18	8
i_{corr}:	*rate of corrosion (mA/cm^2)*	10	10
k:	*corrosion penetration (μm/year)*	11,6	11,6
t:	*time (years)*	50	
T_{ini}:	*Corrosion initiation time in years*	1,91	1,91
$D_{(t)}$:	*reduced steel diameter(mm)*	**12,42**	**2,42**

Figure 12: Automated excel spreadsheet for the remaining steel diameter after 50years.

Reinforcement diameter at the end of ($t-T_{ini}$)

$D_{(t)}=D_i-i_{corr}*k*(t-T_{ini})$

		Values from study	
		Longitudinal bars	Shear links
D_i:	*initial steel diameter (mm)*	18	8
i_{corr}:	*rate of corrosion (mA/cm^2)*	10	10
k:	*corrosion penetration (μm/year)*	11,6	11,6
t:	*time (years)*	75	
T_{ini}:	*Corrosion initiation time in years*	1,91	1,91
$D_{(t)}$:	*reduced steel diameter(mm)*	**9,52**	**-0,48**

Figure 13: Automated excel spreadsheet for the remaining steel diameter after 75years.

Once the process of corrosion has started, the percentage of reduction of the steel reinforcement was calculated as shown in the figure below.

Time dependent loss of steel cross sectional area

$$A(t) = \begin{cases} n.Di^2.\frac{\pi}{4} & for\ t \leq Tini \\ \max\left[n.D(t)^2.\frac{\pi}{4}, 0\right] & for\ t \geq Tini \end{cases}$$

Values from study

n:	*number of steel bars*	12
D_i:	*initial steel diameter (mm)*	18
t:	*time (years)*	**25**
A(t) ≤ T_{ini} (mm):	**3052,08**	
A(t) ≥ T_{ini} (mm):	**2211,28**	
Reduction rate % :	**27,55**	

n:	*number of steel bars*	12
D_i:	*initial steel diameter (mm)*	18
t:	*time (years)*	**50**
A(t) ≤ T_{ini} (mm):	**3052,08**	
A(t) ≥ T_{ini} (mm):	**1453,41**	
Reduction rate % :	**52,38**	

n:	*number of steel bars*	12
D_i:	*initial steel diameter (mm)*	18
t:	*time (years)*	**75**
A(t) ≤ T_{ini} (mm):	**3052,08**	
A(t) ≥ T_{ini} (mm):	**853,98**	
Reduction rate % :	**72,02**	

Figure 14: Automated excel spreadsheet for time-dependent loss of reinforcement cross sectional area.

7.4 Steel ultimate deformation reduction "ε_{su}".

According to Fotopoulou et al. 2013, ductility is taken into consideration hence except from steel area loss, the ultimate deformation of steel affected by corrosion is also presented in this study.

Using the calculation process for moment – curvature of the middle columns with axial loads just as stated in Kombou 2015, the moments and curvature values were obtained at the maximum concrete strain. Furthermore, these values were used as properties of the plastic hinges at the edges of the members using the SAP2000 software.

7.5 Moment vs Curvature methodology

In order to obtain the moment and curvature values, the properties from the following tables were used within the methodology which is described in the following sections. The tables show the reduced steel diameter according to the time of reference as mentioned in section 7.3. The calculations were made in a Microsoft Excel file, in an automated spreadsheet. In those calculations, the reduced steel diameter and steel deformation were taken into account. As seen below, the diameter of the reinforcement, as well as the diameter of the shear links varies for each scenario.

Table 3: Examination data for 25 years.

25 Years		Middle column data		Floor	Axial Force (N)
Constants		b (mm)	425	G	1326500
f_{ck} (MPa)	16	h (mm)	425	1	1320500
E_{c2}	0,002	d (mm)	392,25	2	1131000
E_{cu2}	0,004	d' (mm)	32,75	3	941500
E_s (GPa)	200	cover	20	4	752000
f_{yk} (MPa)	410	φ_{link} (mm)	5	5	562500
ε_y	2,05	φ_{bar} (mm)	15,5	6	373000
E_{uk}	0,05	A_s (mm^2)	2263,16	7	183500

Table 4: Examination data for 50 years.

50 Years		Middle column data		Floor	Axial Force (N)
Constants		b (mm)	425,00	G	1326500
f_{ck} (MPa)	16	h (mm)	425,00	1	1320500
E_{c2}	0,002	d (mm)	396,75	2	1131000
E_{cu2}	0,0035	d' (mm)	28,25	3	941500
E_s (GPa)	200	cover	20,00	4	752000
f_{yk} (MPa)	410	φ_{link} (mm)	2,00	5	562500
ε_y	2,05	φ_{bar} (mm)	12,50	6	373000
E_{uk}	0,05	A_s (mm^2)	1471,88	7	183500

Table 5: Examination data for 75 years.

75 Years			Middle column data			Floor	Axial Force (N)
Constants			b (mm)	425		G	1326500
f_{ck} (MPa)	16		h (mm)	425		1	1320500
E_{c2}	0,002		d (mm)	400		2	1131000
E_{cu2}	0,004		d' (mm)	25		3	941500
E_s (GPa)	200		cover	20		4	752000
f_{yk} (MPa)	410		φ_{link} (mm)	0		5	562500
ε_y	2,05		φ_{bar} (mm)	10		6	373000
E_{uk}	0,05		A_s (mm^2)	942		7	183500

The equations below were used in order to obtain the values of Moment and Curvature.

7.5.1 Concrete strength "fc"

$$\text{for} \quad 0 \le \varepsilon_c \le \varepsilon_{c2} \qquad f_c = f_{ck}\left[1-\left(1-\frac{\varepsilon_c}{\varepsilon_{c2}}\right)^2\right] \tag{6.1}$$

$$\text{for} \quad \varepsilon_{c2} \le \varepsilon_c \le \varepsilon_{cu2} \qquad f_c = f_{ck} \tag{6.2}$$

7.5.2 Cross sectional area "A"

$$\text{for} \quad 0 \le \varepsilon_c \le \varepsilon_{c2} \qquad A = f_{ck}.\left(\frac{{\varepsilon_c}^2}{\varepsilon_{c2}}-\frac{{\varepsilon_c}^3}{3.{\varepsilon_{c2}}^2}\right) \tag{6.3}$$

$$\text{for} \quad \varepsilon_{c2} \le \varepsilon_c \le \varepsilon_{cu2} \qquad A = \frac{2}{3}.f_{ck}.\varepsilon_{c2} + f_{ck}.(\varepsilon_c - \varepsilon_{c2}) \tag{6.4}$$

7.5.3 First moment of cross sectional area "m"

$$\text{for} \quad 0 \le \varepsilon_c \le \varepsilon_{c2} \qquad m = f_{ck}.\left(\frac{2}{3}.\frac{{\varepsilon_c}^3}{\varepsilon_{c2}}-\frac{{\varepsilon_c}^4}{4.{\varepsilon_{c2}}^2}\right) \tag{6.5}$$

$$\text{for} \quad \varepsilon_{c2} \le \varepsilon_c \le \varepsilon_{cu2} \qquad m = \frac{5}{12}.f_{ck}.{\varepsilon_{c2}}^2 + \frac{1}{2}.f_{ck}.({\varepsilon_c}^2 - {\varepsilon_{c2}}^2) \tag{6.6}$$

7.5.4 Average factor "α"

$$\alpha = \frac{A}{\sigma_c.\varepsilon_c} \tag{6.7}$$

Where, $\sigma_c = f_c$

7.5.5 Partial factor "γ"

$$\gamma = 1 - \frac{m}{\varepsilon_c.A} \tag{6.8}$$

7.5.6 Calculation of neutral axis "χ"

$$\text{for} \quad \varepsilon_s > \varepsilon_y \qquad a.f_c.b.\chi - E_s.\frac{d-x}{x}.\varepsilon_c.A_s = N \tag{6.9}$$

$$\text{for} \quad \varepsilon_s < \varepsilon_y \qquad a.f_c.b.\chi - A_s.f_{yk} = N \tag{6.10}$$

7.5.7 Tension / Compression force "Fs"

$$\text{for} \quad \varepsilon_s < \varepsilon_y \qquad F_s = E_s.\varepsilon_s.A_s \tag{6.11}$$

$$\text{for} \quad \varepsilon_s > \varepsilon_y \qquad F_s = f_{yk}.A_s \tag{6.12}$$

Where, $\varepsilon_s = \varepsilon_c.\left(\frac{d-\chi}{\chi}\right)$

7.5.8 Final moment calculation "M"

$$M = \left[F_s.\left(\frac{h}{2} - d'\right) + a.f_c.b.x.\left(\frac{h}{2} - \gamma.x\right)\right]/10^6 \tag{6.13}$$

7.5.9 Curvature "Φ" or "1/R"

$$\Phi = \frac{1}{R} = \frac{\varepsilon_c}{\chi} = \frac{\varepsilon_s}{d-\chi} \tag{6.14}$$

7.6 Limit state of near collapse

The body of the building has the ability to sustain the expected loads of an earthquake and even on some higher levels, without any other safety margins against total collapse (Kombou 2015).

For the strengths of materials, a corrective coefficient factor of 1.35 (KL1) was used (Eurocode 8 – Part 3), which emulates the design based on the practice during the construction time and limited on-site inspection.

According to Eurocode 8-Part 3, the value of the total chord rotation capacity at ultimate state of members under cyclic loading may be calculated as:

$$\Theta um = \frac{1}{\gamma el}.0{,}016(0{,}3^{\nu})\left[\frac{\max(0{,}01;\omega')}{\max(0{,}01;\omega)}.fc\right]^{0{,}225}\left[\min(9,\frac{Lv}{h}\right]^{0{,}35} 25^{\left(a\rho_{sx}\frac{fyw}{fc}\right)}.\left(1{,}25^{100\rho d}\right) \tag{6.15}$$

Where, $\gamma_{el} = 1.5$

The value of the plastic part of the chord rotation capacity of members under loading is calculated as follows:

$$\Theta^{pl}um = \frac{1}{\gamma el}.0{,}0145(0{,}25^{\nu})\left[\frac{\max(0{,}01;\omega')}{\max(0{,}01;\omega)}\right]^{0{,}3}.fc.\left[\min(9,\frac{Lv}{h}\right]^{0{,}35}.25^{\left(a\rho_{sx}\frac{fyw}{fc}\right)}.\left(1{,}275^{100\rho d}\right) \quad (6.16)$$

Parameters:

γ_{el} = 1.5 for Θ_{um}

γ_{el} = 1.8 for Θ_{um}^{pl}

$$\nu = \frac{N}{b.h.f_c} \quad (6.17)$$

$$\omega = \frac{A_s}{b.d}.\frac{f_y}{f_c} \quad (6.18)$$

$$\omega' = \frac{A'_s}{b.d}.\frac{f_y}{f_c} \quad (6.19)$$

$$L_v = 0{,}5h \quad (6.20)$$

$$a = \left(1 - \frac{S_h}{2.b_o}\right).\left(1 - \frac{S_h}{2.h_o}\right).\left(1 - \frac{\Sigma {b_i}^2}{6.h_o.b_o}\right) \quad (6.21)$$

$$\rho_{sx} = \frac{A_{sw}}{b_w.S_h} \quad (6.22)$$

7.7 Cyclic shear resistance "V_R"

There is a possibility that columns might fail due to shear before bending failure. For that reason, the following expression was used to obtain the shear strength of the columns.

$$VR = \frac{1}{\gamma el}.\left[\frac{h-x}{2Lv}\min(N; 0{,}55.Ac.fc) + (1 - 0{,}05.\min(5; \mu_{\Delta}^{pl})).\left[0{,}16.\max(0{,}5; 100\rho_{tot})\left(1 - 0{,}16.\min\left(5; \frac{Lv}{h}\right)\right)\sqrt{fc}.Ac + Vw\right]\right] \quad (6.23)$$

Where, γ_{el} = 1.15 for steel

$$\mu_{\Delta}^{pl} = \mu\Delta - 1 = \Theta/\Theta y = \Theta plum/\Theta y \quad (6.24)$$

$$\Theta_y = \Theta_{um} - \Theta_{um}^{pl} \quad (6.25)$$

$$V_w = \rho_w.b_w.z.f_{yw} \quad (6.26)$$

7.8 Calculation results

The following tables present the results from the methodology in section 7.7 for the middle columns.

Table 6: 25 Years - excel spreadsheet display of formulae results

25 Years					
Floor	Θum	Θ^{pl}um	M (kNm)	Φ or (1/R) (mm^{-1})	$V_{R\,(kN)}$(6.23)
G	0,0138	0,0088	213,36	1,12E-05	207,24
1	0,0139	0,0088	214,07	1,12E-05	201,85
2	0,0154	0,0100	236,28	1,18E-05	188,35
3	0,0171	0,0113	258,13	1,24E-05	174,68
4	0,0191	0,0127	279,78	1,30E-05	160,86
5	0,0212	0,0144	301,36	1,37E-05	146,87
6	0,0236	0,0163	314,92	1,44E-05	132,71

Table 7: 50 Years - excel spreadsheet display of formulae results

50 Years					
Floor	Θum	Θ^{pl}um	M (kNm)	Φ or (1/R) (mm^{-1})	$V_{R\,(kN)}$(6.23)
G	0,0137	0,0087	205,31	1,16E-05	163,56
1	0,0138	0,0087	205,93	1,17E-05	163,14
2	0,0153	0,0099	225,24	1,24E-05	149,81
3	0,0171	0,0112	244,06	1,32E-05	136,32
4	0,0190	0,0126	260,47	1,41E-05	122,68
5	0,0211	0,0143	259,46	1,50E-05	108,89
6	0,0235	0,0162	243,88	1,60E-05	94,94

Table 8: 75 Years – excel spreadsheet display of formulae results

75 Years					
Floor	Θum	Θ^{pl}um	M (kNm)	Φ or (1/R) (mm^{-1})	$V_{R\,(kN)}$(6.23)
G	0,0137	0,0087	195,26	1,22E-05	138,17
1	0,0138	0,0087	195,77	1,22E-05	137,76
2	0,0153	0,0099	211,51	1,32E-05	124,52
3	0,0170	0,0112	220,83	1,42E-05	111,14
4	0,0190	0,0126	214,31	1,54E-05	97,62
5	0,0211	0,0143	202,45	1,66E-05	83,95
6	0,0235	0,0161	185,71	1,80E-05	70,14

7.9 Graphs

The graph below shows the reduction of the strength of the columns in shearing while the years of life of the building are increasing. The method used to obtain the values of the shear forces for the graph was obtained from Eurocode 8.3 and is presented in section 7.7.

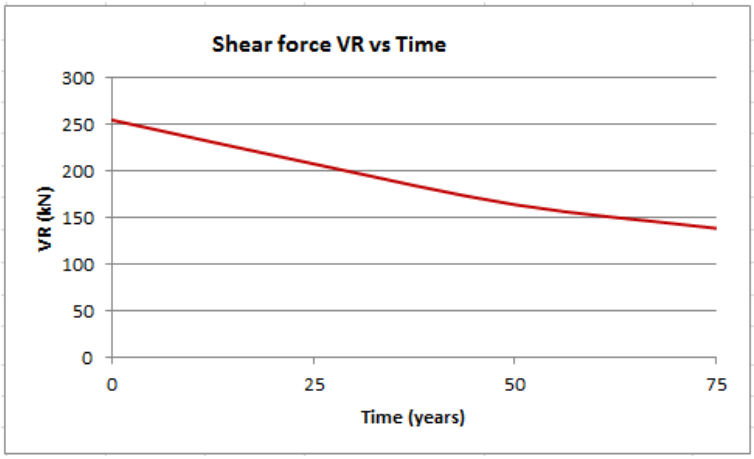

Figure 15: Decrease of column strength over time

The moment – curvature relationship was produced for all floors of the structural model. The graphs below show the relationship for the third floor.

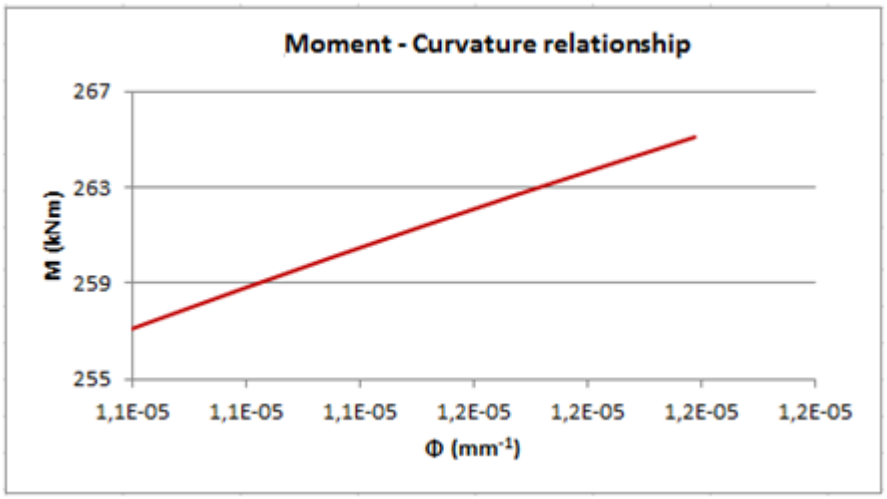

Figure 16: Moment-Curvature for the third floor after 0 years

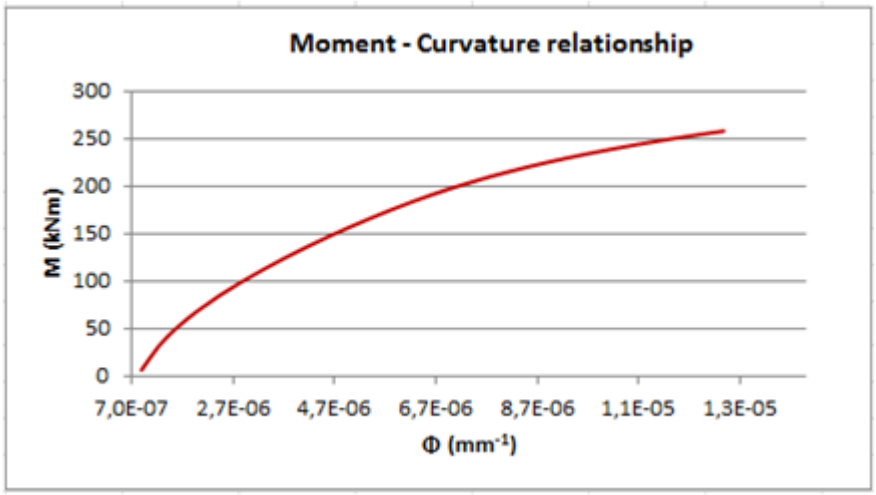

Figure 17: Moment-Curvature for the third floor after 25 years

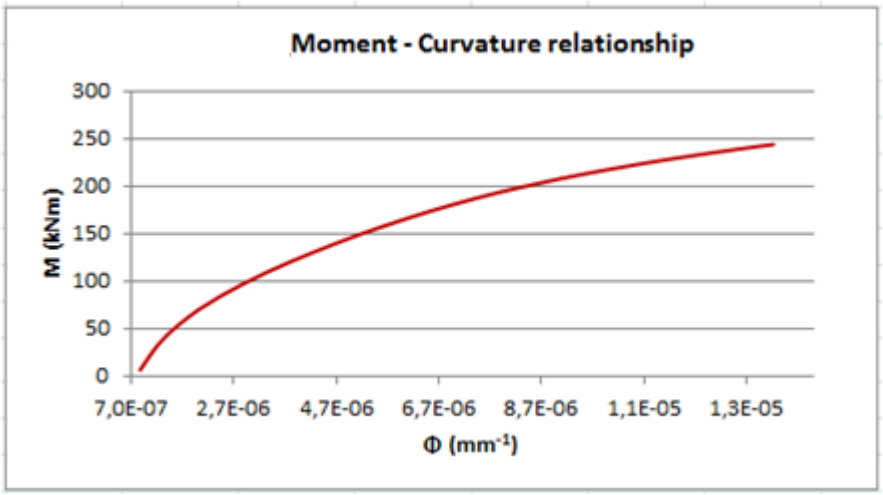

Figure 18: Moment-Curvature for the third floor after 50 years

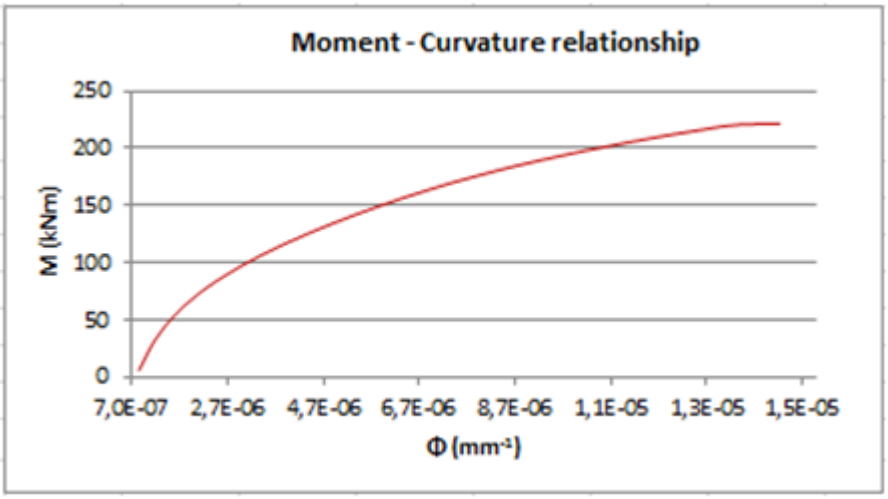

Figure 19: Moment-Curvature for the third floor after 75 years

8 Pushover analysis of a 2D multi-storey building

The maximum forces acting at the base of the middle columns were monitored and then compared to the forces calculated in section 7.8 to finally determine the type of failure. The figures below show the step by step procedure followed in the software. The analysis options were set to XZ plane (with Ux, Uz, and Ry DOFs) and the material properties were define as seen in Figure 20.

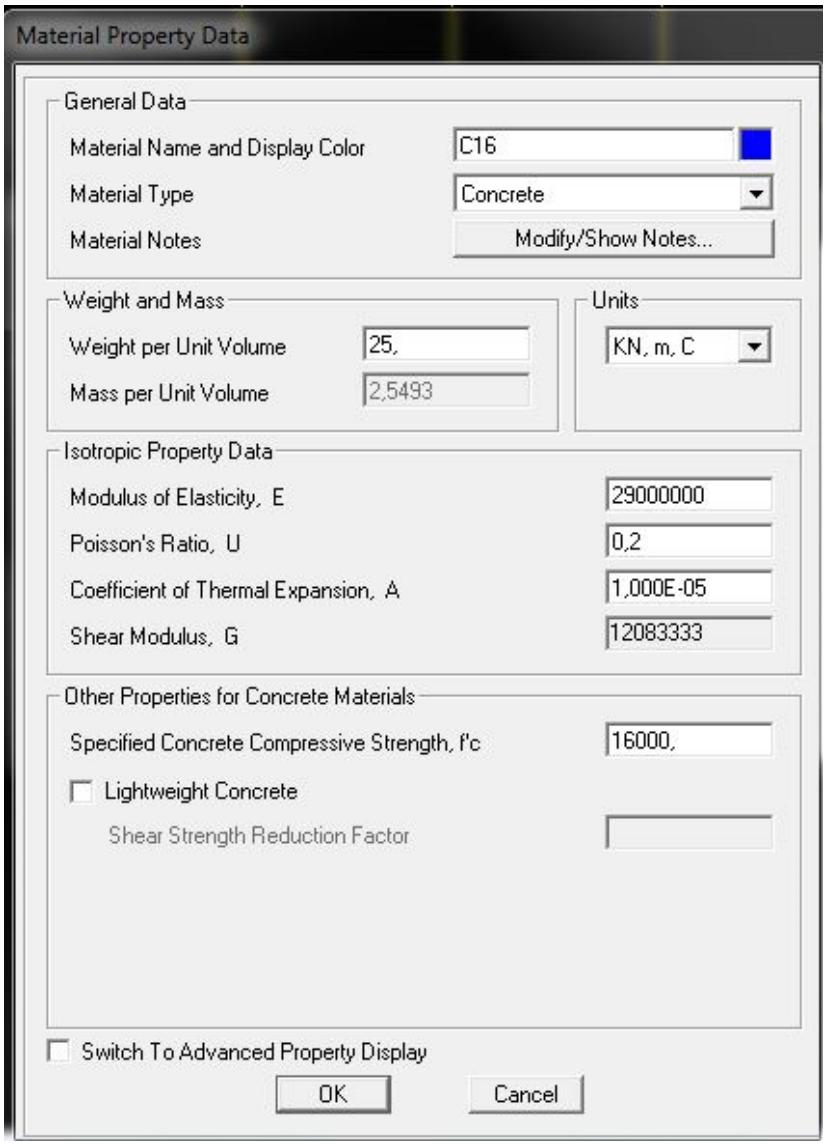

Figure 20: SAP2000 - Concrete Properties

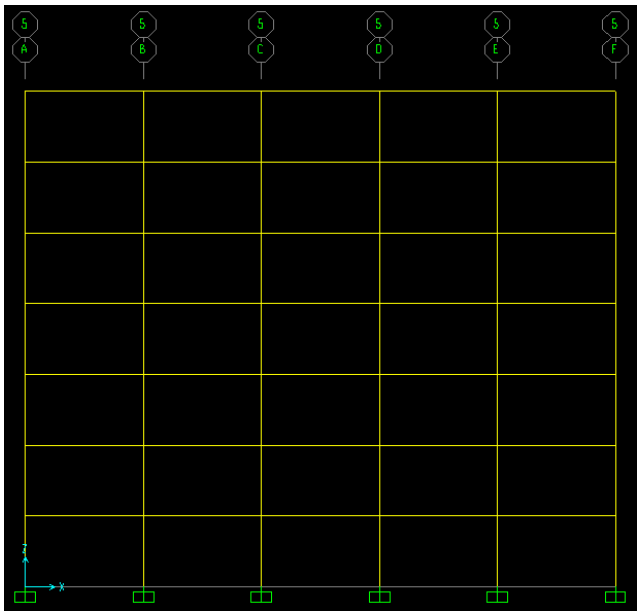

Figure 21: SAP2000 – 2D Model with fixed ends

After the design of the sections, the frame was modeled as seen in Figure 21 with the restraints as fixed ends.

8.1 Hinge Properties

Plastic hinges were placed at both ends of every member, to monitor the behavior of the sections during the pushover analysis on every floor. The properties of the hinges, as shown below in Figure 22, have been regulated according to the moment-curvature values from the calculations in section 7.8, while the deformation of steel was taken into account.

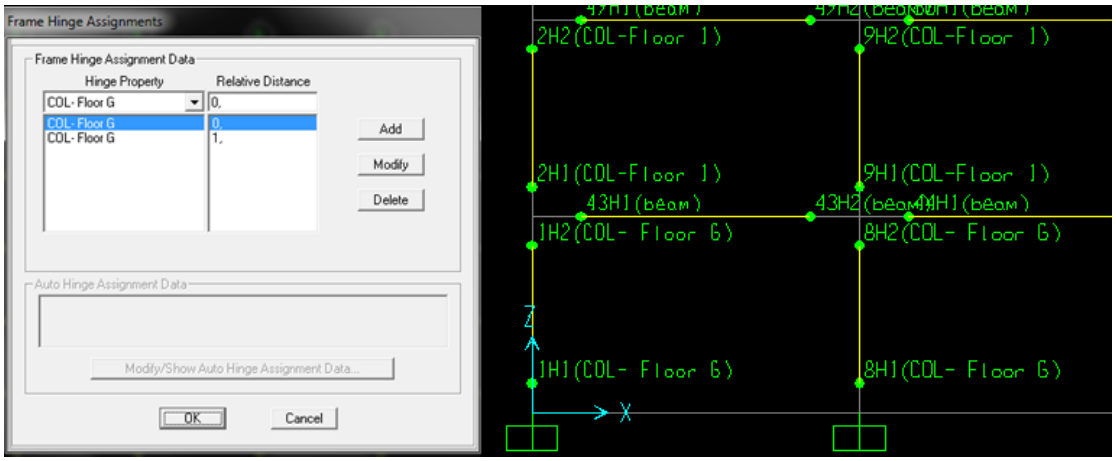

Figure 22: SAP2000 – Assign hinges properties.

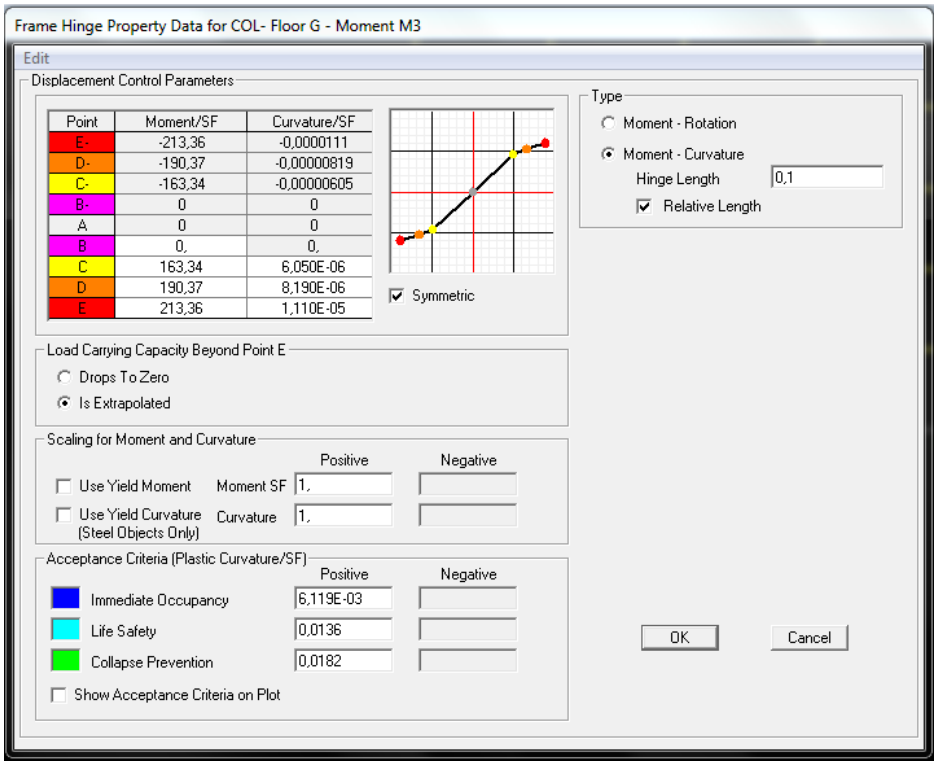

Figure 23: SAP2000 – Example of hinge properties on columns for G-Floor sections for the period of 25 years.

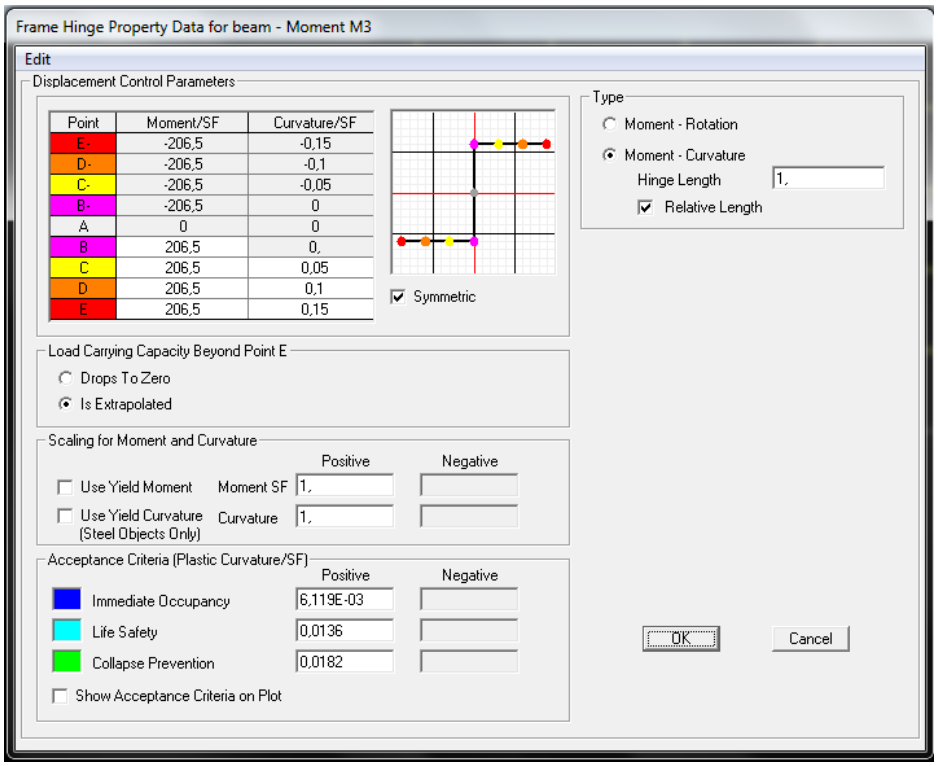

Figure 24: SAP2000 – Example of hinge properties on beams for G-Floor sections for the period of 25 years.

8.2 Load patterns

The loading patterns of the frame were as follows: distributed Dead Load (DL)= 32.5kN/m and Live Load (LL)= 10kN/m (Kombou 2015), while a triangular pattern lateral load starting at the value of 1 at the top left joint (node 8) assigned partially deducted downwards at each floor level for the pushover analysis as seen in Figure 25.

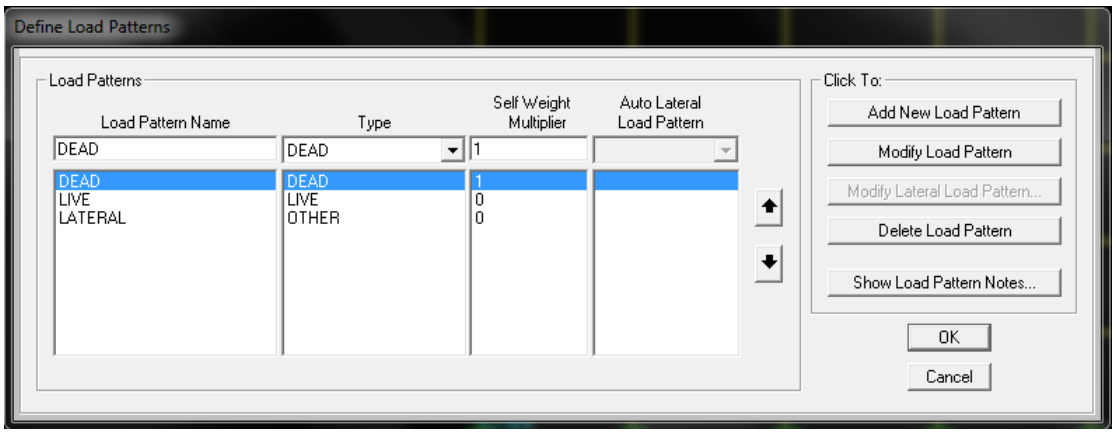

Figure 25: SAP2000 – Load Patterns

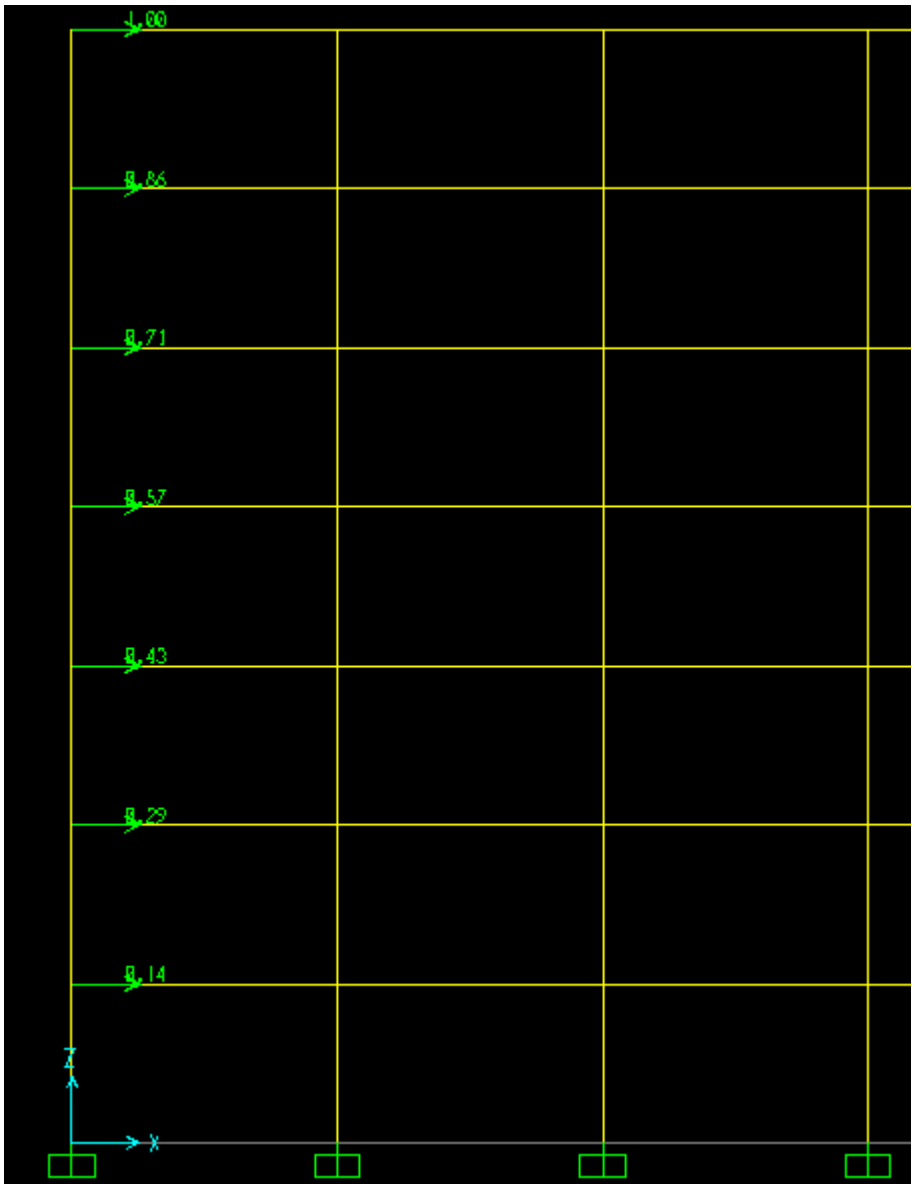

Figure 26: SAP2000 – Triangular lateral load

8.3 Results of the Pushover analysis

In the graphical representations below it is shown more precisely the way the columns fail. The values stated in the graphs represent the maximum shear forces the columns can withstand for the four periods. As age of the building increases, the shear force that it resists is reducing and precedes flexural failure of the structure.

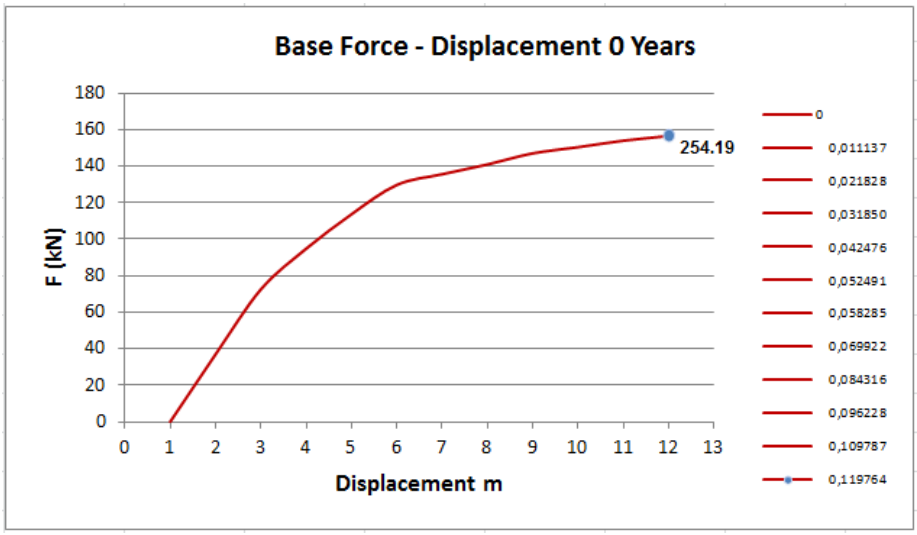

Figure 27: Comparative Analysis of the Maximum Shear Force at Collapse – 0 years

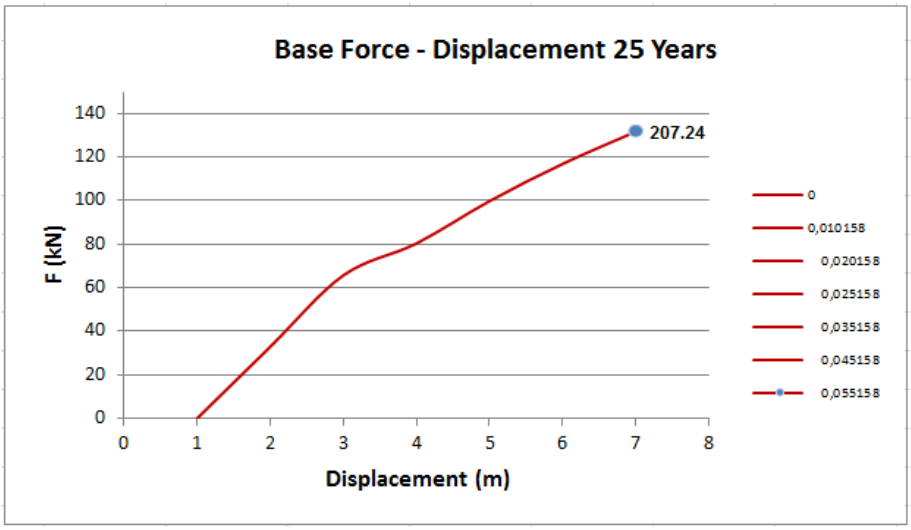

Figure 28: Comparative Analysis of the Maximum Shear Force at Collapse – 25 years

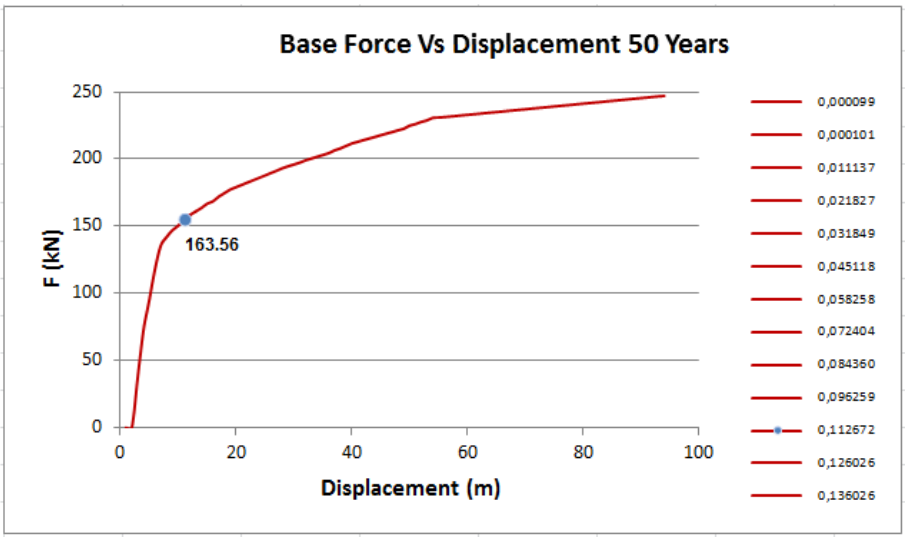

Figure 29: Comparative Analysis of the Maximum Shear Force at Collapse – 50 years

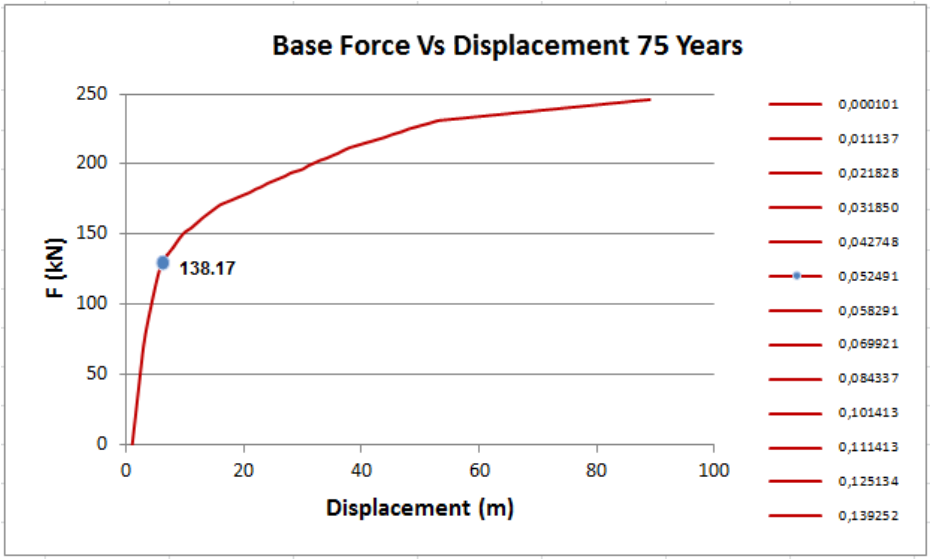

Figure 30: Comparative Analysis of the Maximum Shear Force at Collapse – 75 years

9 Time history analysis of a 2D multi-storey building

With the time history analysis based on the accelerograms presented in section 6.1, the seismic evaluation of the capacity of the structure through time is further examined. The purpose of the analysis is to show the maximum seismic acceleration value that causes the shear failure of the columns.

9.1 Time history function

The same model that was used for the pushover analysis has been also used for the time history analysis with an addition of the seismic input as shown in the figure below.

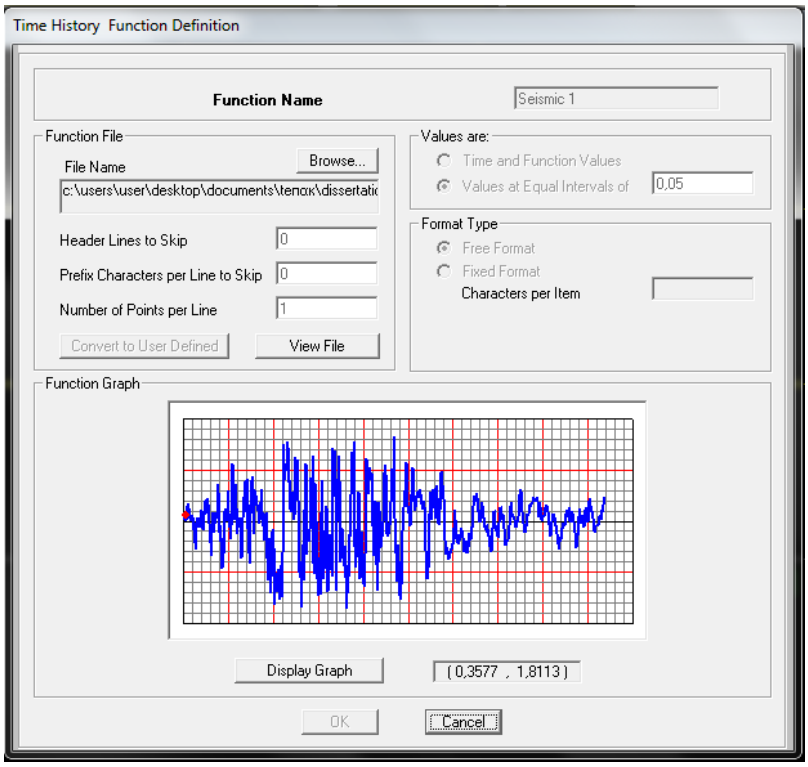

Figure 31: Seismic file input for Seismic 1

The analysis was run for four time periods, namely, 0, 25, 50, and 75 years and with six seismic inputs for each one. In addition, the scale factor was changed (see figure 28) so as to obtain the closest value that reaches the maximum shear force at the base as it was found in the pushover analysis. The closest value to the shear force gives the acceleration that causes the failure of the section.

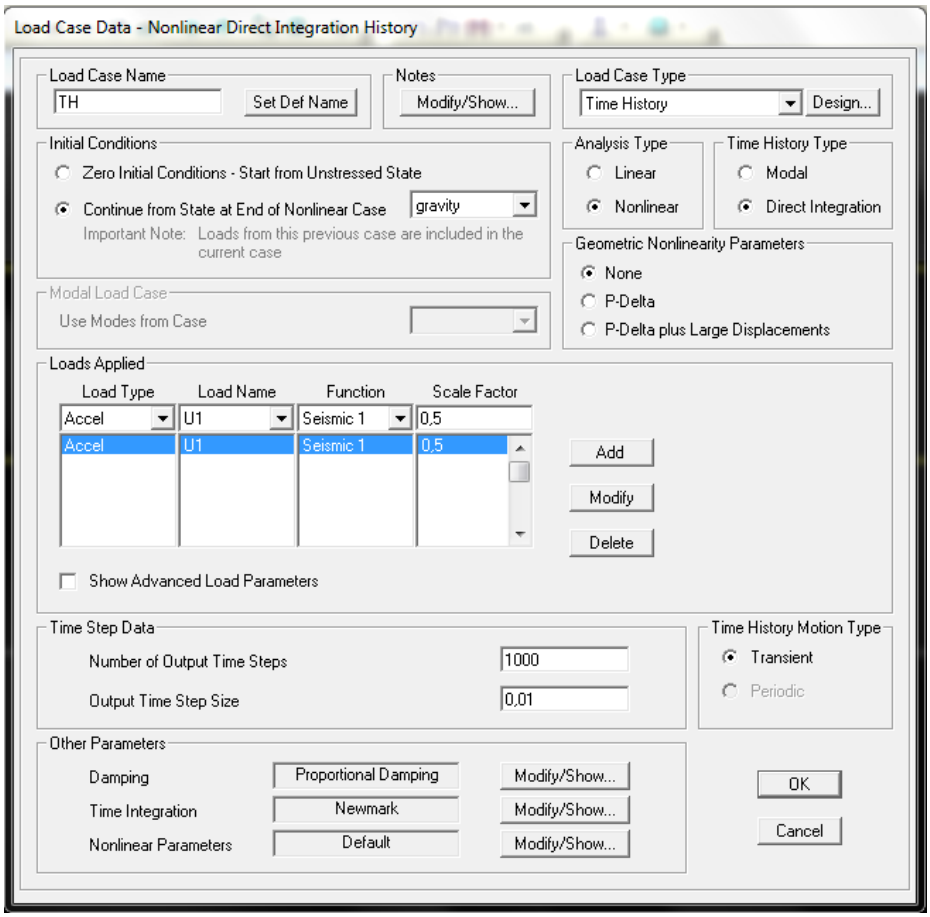

Figure 32: Load case of the non-linear time history analysis

9.2 Results of the time history analysis

The resulted accelerations from the time history analysis are shown in red in the tables below. The tables also show in summary, the overall strength decrease of the model for the four periods examined for all six seismic inputs

Table 9: Result for Friuli seismic record (PGA = 0.248g)

SEISMIC 1 - 0,248g								
0 Years					25 Years				
Time History analysis results			EC8-Part3		Time History analysis results			EC8-Part3	
Scale	Acceleration	Base Shear (kN)	VR (kN)(6.23)		Scale	Acceleration	Base Shear (kN)	VR (kN)(6.23)	
0,248*0,8=	0,19g	453,36	>		0,248*0,6=	0,15g	215,33	>	
0,248*0,7=	0,17g	243,31			0,248*0,5=	0,124g	205,23		
0,248*0,6=	0,15g	215,33	<	254,19kN	0,248*0,4=	0,099g	173,88	<	207,24kN
0,248*0,5=	0,124g	205,84			0,248*0,3=	0,074g	163,02		
0,248*0,4=	0,099g	178,62			0,248*0,2=	0,049g	102,28		
50 Years					75 Years				
Time History analysis results			EC8-Part3		Time History analysis results			EC8-Part3	
Scale	Acceleration	Base Shear (kN)	VR (kN)(6.23)		Scale	Acceleration	Base Shear (kN)	VR (kN)(6.23)	
0,248*0,5=	0,124g	204,91	>		0,248*0,5=	0,124g	240,36		
0,248*0,4=	0,099g	165,35			0,248*0,4=	0,099g	207,66	>	
0,248*0,3=	0,074g	163,06		163,56kN	0,248*0,3=	0,074g	194,88		138,17kN
0,248*0,2=	0,049g	92,08	<		0,248*0,2=	0,049g	186,47		
0,248*0,1=	0,024g	60,45			0,248*0,1=	0,024g	128,47	<	

Table 10: Result for Montenegro seismic record (PGA = 0.25g)

SEISMIC 2 - 0,25g								
0 Years					25 Years				
Time History analysis results			EC8-Part3		Time History analysis results			EC8-Part3	
Scale	Acceleration	Base Shear (kN)	VR (kN)(6.23)		Scale	Acceleration	Base Shear (kN)	VR (kN)(6.23)	
0,25*0,8=	0,2g	265,89	>		0,25*0,7=	0,175g	233,28	>	
0,25*0,7=	0,175g	230,10			0,25*0,6=	0,15g	200,86		
0,25*0,6=	0,15g	196,43	<	254,19kN	0,25*0,5=	0,125g	175,52	<	207,24kN
0,25*0,5=	0,125g	191,35			0,25*0,4=	0,1g	151,56		
0,25*0,4=	0,1g	156,23			0,25*0,3=	0,075g	141,50		
50 Years					75 Years				
Time History analysis results			EC8-Part3		Time History analysis results			EC8-Part3	
Scale	Acceleration	Base Shear (kN)	VR (kN)(6.23)		Scale	Acceleration	Base Shear (kN)	VR (kN)(6.23)	
0,25*0,5=	0,125g	189,60	>		0,25*0,5=	0,125g	184,67		
0,25*0,4=	0,1g	154,33			0,25*0,4=	0,1g	158,46	>	
0,25*0,3=	0,075g	141,62	<	163,56kN	0,25*0,3=	0,075g	151,39		138,17kN
0,25*0,2=	0,05g	103,03			0,25*0,2=	0,05g	105,91	<	
0,25*0,1=	0,025g	54,69			0,25*0,1=	0,025g	62,71		

Table 11: Result for Kalamata seismic record (PGA = 0.239g)

SEISMIC 3 -0, 239g									
0 Years					25 Years				
Time History analysis results			EC8-Part3		Time History analysis results			EC8-Part3	
Scale	Acceleration	Base Shear (kN)	VR (kN)(6.23)		Scale	Acceleration	Base Shear (kN)	VR (kN)(6.23)	
0,239*0,9=	0,216g	298,58	>		0,239*0,5=	0,12g	213,65	>	
0,239*0,8=	0,192g	245,30			0,239*0,4=	0,096g	192,17		
0,239*0,7=	0,168g	243,65	<	254,19kN	0,239*0,3=	0,072g	179,38	<	207,24kN
0,239*0,6=	0,144g	223,31			0,239*0,2=	0,048g	153,38		
0,239*0,5=	0,12g	202,03			0,239*0,1=	0,024g	130,07		
50 Years					75 Years				
Time History analysis results			EC8-Part3		Time History analysis results			EC8-Part3	
Scale	Acceleration	Base Shear (kN)	VR (kN)(6.23)		Scale	Acceleration	Base Shear (kN)	VR (kN)(6.23)	
0,239*0,5=	0,12g	215,46			0,239*0,3=	0,072g	171,39		
0,239*0,4=	0,096g	192,51	>		0,239*0,2=	0,048g	162,32	>	
0,239*0,3=	0,072g	177,65		163,56kN	0,239*0,1=	0,024g	140,96		138,17kN
0,239*0,2=	0,048g	153,39	<		0,239*0,09=	0,021g	139,40		
0,239*0,1=	0,024g	141,92			0,239*0,08=	0,019g	109,85	<	

Table 12: Result for Loma Prieta seismic record (PGA = 0.254g)

SEISMIC 4 - 0,254g									
0 Years					25 Years				
Time History analysis results			EC8-Part3		Time History analysis results			EC8-Part3	
Scale	Acceleration	Base Shear (kN)	VR (kN)(6.23)		Scale	Acceleration	Base Shear (kN)	VR (kN)(6.23)	
0,254*0,9=	0,228g	389,27	>		0,254*0,6=	0,152g	229,71	>	
0,254*0,8=	0,203g	235,99			0,254*0,5=	0,127g	204,41		
0,254*0,7=	0,177g	192,89	<	254,19kN	0,254*0,4=	0,102g	180,10	<	207,24kN
0,254*0,6=	0,152g	187,83			0,254*0,3=	0,076g	169,83		
0,254*0,5=	0,127g	183,90			0,254*0,2=	0,05g	109,60		
50 Years					75 Years				
Time History analysis results			EC8-Part3		Time History analysis results			EC8-Part3	
Scale	Acceleration	Base Shear (kN)	VR (kN)(6.23)		Scale	Acceleration	Base Shear (kN)	VR (kN)(6.23)	
0,254*0,5=	0,127g	213,83	>		0,254*0,5=	0,127g	197,33		
0,254*0,4=	0,102g	199,89			0,254*0,4=	0,102g	190,99	>	
0,254*0,3=	0,076g	160,71		163,56kN	0,254*0,3=	0,076g	172,74		138,17kN
0,254*0,2=	0,05g	140,75	<		0,254*0,2=	0,05g	102,11	<	
0,254*0,1=	0,025g	68,08			0,254*0,1=	0,025g	66,15		

Table 13: Result for Imperial Valley 1979 seismic record (PGA = 0.268g)

SEISMIC 5 - 0,268g									
0 Years					25 Years				
Time History analysis results			EC8-Part3		Time History analysis results			EC8-Part3	
Scale	Acceleration	Base Shear (kN)	VR (kN)(6.23)		Scale	Acceleration	Base Shear (kN)	VR (kN)(6.23)	
0,268*0,8=	0,214g	271,72	>		0,268*0,7=	0,187g	227,25	>	
0,268*0,7=	0,187g	233,70	<	254,19kN	0,268*0,6=	0,160g	197,75	<	207,24kN
0,268*0,6=	0,160g	203,36			0,268*0,5=	0,134g	194,85		
0,268*0,5=	0,134g	195,76			0,268*0,4=	0,107g	160,79		
0,268*0,4=	0,107g	160,00			0,268*0,3=	0,080g	135,42		
50 Years					75 Years				
Time History analysis results			EC8-Part3		Time History analysis results			EC8-Part3	
Scale	Acceleration	Base Shear (kN)	VR (kN)(6.23)		Scale	Acceleration	Base Shear (kN)	VR (kN)(6.23)	
0,268*0,5=	0,134g	179,37	>		0,268*0,5=	0,134g	190,37	>	
0,268*0,4=	0,107g	163,04	<	163,56kN	0,268*0,4=	0,107g	161,16		138,17kN
0,268*0,3=	0,080g	141,37			0,268*0,3=	0,080g	141,99		
0,268*0,2=	0,053g	139,49			0,268*0,2=	0,053g	138,68		
0,268*0,1=	0,026g	82,26			0,268*0,1=	0,026g	88,29	<	

Table 14: Result for Imperial Valley 1940 seismic record (PGA = 0.255g)

SEISMIC 6 - 0,255g									
0 Years					25 Years				
Time History analysis results			EC8-Part3		Time History analysis results			EC8-Part3	
Scale	Acceleration	Base Shear (kN)	VR (kN)(6.23)		Scale	Acceleration	Base Shear (kN)	VR (kN)(6.23)	
0,255*0,8=	0,204g	288,38	>		0,255*0,5=	0,127g	254,97	>	
0,255*0,7=	0,178g	231,06	<	254,19kN	0,255*0,4=	0,102g	178,36	<	207,24kN
0,255*0,6=	0,153g	198,50			0,255*0,3=	0,076g	157,96		
0,255*0,5=	0,127g	186,52			0,255*0,2=	0,051g	155,65		
0,255*0,4=	0,102g	179,48			0,255*0,1=	0,025g	101,61		
50 Years					75 Years				
Time History analysis results			EC8-Part3		Time History analysis results			EC8-Part3	
Scale	Acceleration	Base Shear (kN)	VR (kN)(6.23)		Scale	Acceleration	Base Shear (kN)	VR (kN)(6.23)	
0,255*0,5=	0,127g	254,00	>		0,255*0,5=	0,127g	236,92	>	
0,255*0,4=	0,102g	184,78			0,255*0,4=	0,102g	202,72		
0,255*0,3=	0,076g	155,49	<	163,56kN	0,255*0,3=	0,076g	159,82		138,17kN
0,255*0,2=	0,051g	153,89			0,255*0,2=	0,051g	148,69		
0,255*0,1=	0,025g	96,85			0,255*0,1=	0,025g	117,87	<	

Table 15: Seismic acceleration at collapse

Decrease %	T (years)	Seismic 1(g)	Seismic 2(g)	Seismic 3(g)	Seismic 4(g)	Seismic 5(g)	Seismic 6(g)
0	0	0,17	0,2	0,192	0,203	0,214	0,178
27	25	0,124	0,15	0,12	0,127	0,16	0,102
40	50	0,074	0,1	0,048	0,076	0,107	0,076
67	75	0,024	0,075	0,021	0,05	0,053	0,051

10 Discussion

Based on corrosion modeling, the loss of steel area increases significantly over a given time period. In the transition between 0 to 25 years, the area of steel lost is almost 30%, at 50 years it is 50% and at 70 years it is 70%.

Examining the results of the pushover analysis, it appears that column shear failure occurs within 25 and 50 years of a structure's life, while taking into account the change in the deformation capacity of the reinforcement. The pushover analysis was used in order to observe the type of collapse that will take place in the structure. Usually that failure is shear, except from some cases where columns fail due to the decreased reinforcement or by being unable to withstand the axial load and crashing occurs before yielding. By deriving the moment – curvature relationships for the column sections and the seismic load combinations as shown in section 7.9, it was shown that, in some cases, due to high axial force demand in columns, and the low percentage of main reinforcement after the bar deterioration from corrosion, flexural bar yielding is not achieved prior to the attainment of the crushing strain in concrete (ec=0.0035). This failure mode is not as common as the shear one, but, based on the results; it should also be addressed due to its brittle nature. In the cases of longer time period such as 50 and 75 years the columns fail in shear mainly due to the very limited shear reinforcement (links) capacity. This can be seen in the Figures in section 8.3 where the shear force indicated on the graphs occurs before concrete reaches its maximum strain capacity and steel reinforcement its flexural yielding.

In the figure below and for the case of the 25y period, the maximum shear force on columns of the first floor from the seismic combination is at lower levels compared to the force at the shear demand. This is not the case though, for the 50y period since a considerable decrease in the shear capacity is observed resulting to the point where shear failure precedes the crushing failure.

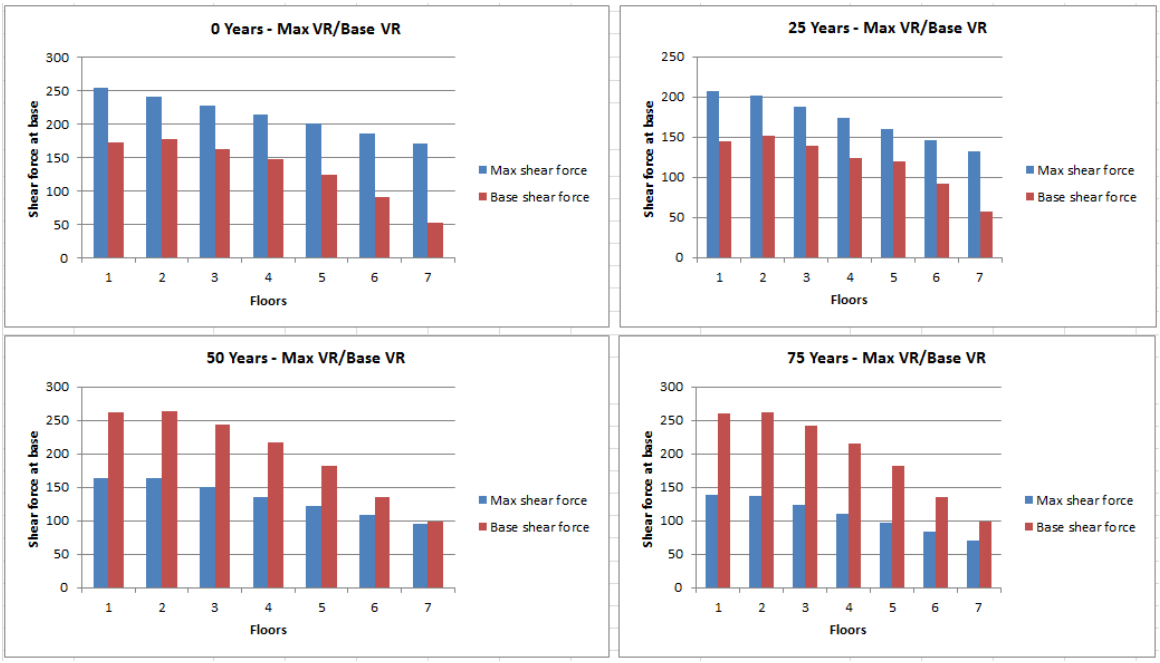

Figure 33: Relationship between maximum bearing shear force and base shear force for each floor.

Based on the results of the time history analysis, it is observed that there is a significant decrease in between the scenarios for a specific earthquake. All earthquake data used in the study follow a similar pattern. The decrease will play a vital role in a probable earthquake of 0.1g, which it will cause shear failure. In the last 30 years there have been earthquakes with higher accelerations in the area of Cyprus. The reason for not having severe damages when earthquakes occurred in the past is because the structures were at the point between 0 to 25 years. Adding a decade to those structures brings them in the present which means that they are entering a critical zone from this point onward.

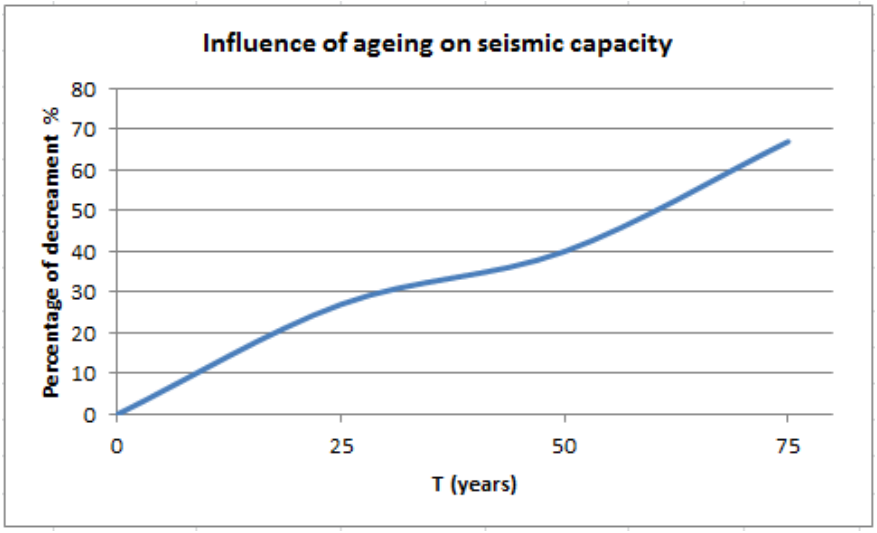

Figure 34: The influence of aging on seismic capacity, Friuli 1976.

The results in section 9.2, show that the members fail due to shearing at fairly low accelerations. Moreover, earthquakes of such accelerations are statistically to occur every ten years. The time to enhance the capacity of aged buildings that have corrosion problems must be within ten years.

Because of the diversity in earthquakes, a mean value was determined to show the results more globally. This is a relationship that links the amount in change of acceleration that failure occurs vs. time. While time passes, the acceleration that causes failure is decreasing.

Having analysed the structural model as described in section 7.2, the decrease in strength is acknowledged. From the results of this study, a 67% of strength reduction is given by the figure below. Furthermore, the equation $\gamma = 0.229e^{-0.02x}$ as seen on the graph is given by the relationship that links the acceleration to the time.
This relationship shows how the seismic acceleration is changing versus time.

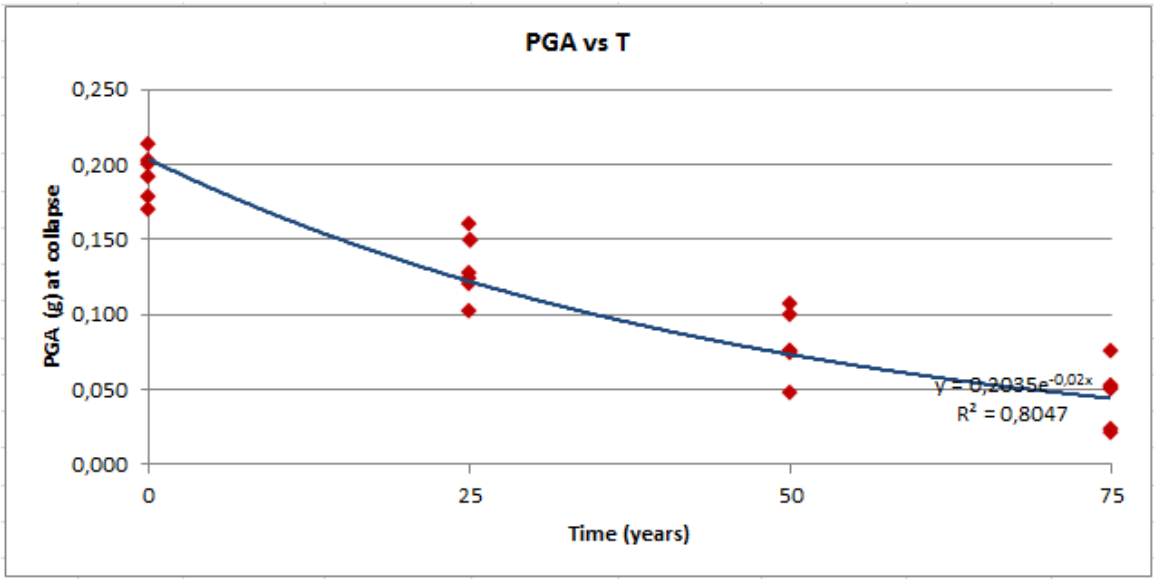

Figure 35: Relation between the seismic acceleration at failure with time

In this case, there is a steady reduction of the seismic capacity of the structure, which just after the 25y margin, leads to a drop of the expected seismic demand that the structure can resist to a value below 0.1g for all records. This pga is considerably lower than the design hazard map for Cyprus used for the design of new buildings in Eurocode 8-part1. It is also lower than the maximum recorded acceleration in Limassol since 1995 when the network was installed, which was 0.164g (Kyriakides, 2007). It is thus evident that whilst buildings which were 25 years of age during the 1996 earthquake might have been able to withstand an

acceleration of 0.164g, without significant damages, the allowable seismic demand has considerably reduced since, and will lead to exceedance of the column's capacity if similar earthquakes were to occur again. Analyzing 50 years later, a typical building that was built before a certain period, according to previous regulations and data, the reduced strength seems to be around 50%, which is very important to be acknowledged.

Conclusion

This study examined the response of an existing building for the time-varying vulnerability of the aging phenomenon. The two main phenomena which were examined in more depth were the steel area loss and its maximum deformation.

Based on the model used, the reinforcement starts to corrode almost 2 years after its construction. The initiation of corrosion was based on the water/cement ratio of 0.45.

The findings state that the steel diameter was reduced to 15.32mm from 18mm for the 25y scenario. The steel diameter for the 50y scenario was reduced to 12.42mm and to 9.52mm for the 75y scenario.

Having considered the steel area loss, it was also reasonable to look at moment – curvature relationship after applying load to the corrosion model. Then the maximum shear resistance of the columns was obtained as seen in section 7.8. It can be seen from the above that shear failure occurs before crushing failure.

In the final analysis, the results present the accelerations that force the columns to fail for the four scenarios. The procedure of time history analysis was repeated for six seismic records as seen in section 6. In short, the results show acceleration values, around 0.1g that comes close to the maximum base shear that causes the column to collapse.

It is a fact that there are RC buildings in Cyprus that survived previous earthquakes with no relative damages. As a rule, people have the impression that undamaged buildings after struck by earthquakes would behave similarly when possible future earthquakes occur. This impression however, neglects the impact of corrosion as well as the deformation of the reinforcement on the RC structures. The results from this study certainly suggest that it is important to consider retrofitting of the above structures.

Furthermore, there is still room for future research in various aspects of this study. Firstly, effective testing is needed for tall structures to possibly determine the role of geometry of the members on strength deterioration.

Further, the development of new construction materials that are resistant to corrosion would increase the life and durability of structures. Construction companies, as well as engineers, should, therefore, employ construction materials that are not prone to corrosion. It will also enhance construction in coastal areas with a minimum risk of corrosion.

REFERENCES

Angst,U., (2011). “Chloride Induced reinforcement corrosion in concrete” Concept of critical chloride content –methods and mechanisms, Doctoral Thesis, Norwegian University of Science and Technology Faculty of Engineering Science and Technology Department of Structural Engineering.

CEB-FIB Task Group5.6 (2006). Model Code for Service Life Design, Fib Bulletin, 34. Switzerland.

Choe, D. E., Gardoni, P., Rosowsky, D., & Haukaas, T. (2009). “Seismic fragility estimates for reinforced concrete bridges subject to corrosion”. Structural Safety, 31(4), 275-283.

Coronelli, D., & Gambarova, P. (2004). “Structural assessment of corroded reinforced concrete beams: modeling guidelines”. Journal of Structural Engineering, 130(8), 1214-1224.

Cyprus Standard. (2005) CYS EN1998-3:2005. Design of Structures for earthquakes resisance-Part 3: Assessment and retrofitting of buildings. Cyprus organization for Standardisation.

Fotopoulou, S. D., Karapetrou, S. T., & Pitilakis, K. D. (2012). “Seismic vulnerability of RC buildings considering SSI and aging effects”, in proceedings of the 15WCEE international conference, LISBOA.

Fotopoulou, S. D., Karapetrou, S. T., & Pitilakis, K. D. (2013). “Consideration of aging effects on the time-dependent seismic vulnerability assessment of RC buildings”, Vienna Congress on Recent Advances in Earthquake and Structural Dynamics, Vienna, Austria.

Ghosh, J. and Padgett, J.E. (2010). “Aging considerations in the development of time-dependent seismic fragility curves”. Journal of Structural Engineering, 136 (12), 1497-1511.

Hooton R.D, Stanish, K.D, Thomas, M.D.A. (2001). “Testing the chloride Penetration Resistance of concrete: A literature review”, Department of Civil Engineering, University of Toronto, Ontario, Canada.

Kombou, M. (2015). "Επίδραση διάβρωσης χάλυβα σε υφιστάμενες κατασκευές οπλισμένου σκυροδέματος", Postgraduate Thesis. Faculty of Engineering and Technology, Department of Civil Engineering and Geomatics, Cyprus University of Technology.

Kyriakides, N. (2007). "Vulnerability of RC buildings and risk assessment for Cyprus", Doctoral Thesis, Faculty of Engineering, University of Sheffield.

Mohammed A., Ahmed A. and Maekawa K. (2014). "AMS14, Seismic Evaluation of Coastal RC Buildings Vulnerable to an Airborne Chloride Environment", Department of Structural Engineering, Cairo University, Giza, Egypt

Neville, A.M., (1995). "Properties of concrete", 5th Ed., Longman, Essex.

Porter, K. (2015). "A beginner's guide to Fragility, Vulnerability, and Risk", PHD Study. University of Colorado Boulder and SPA Risk, Denver CO USA.

Ramamoorthy, S. K., Gardoni, P., & Bracci, J. M. (2007). "Seismic Fragility Estimates for Reinforced Concrete Buildings". Mid-America Earthquake Center.

Rodriquez, J. and Andrade, C. (2001). "CONTECVET – A validated users manual for assessing the residual service life of concrete structures", GEOCISA. Madrid, Spain.

Simioni, P. (2009). *Seismic response of reinforced concrete structures affected by reinforcement corrosion.* PhD thesis. Faculty of Architecture, Civil Engineering and Environmental Sciences University of Braunschweig, Institute of Technology and the Faculty of Engineering University of Florence.

Stewart, M. G. (2004). Spatial variability of pitting corrosion and its influence on structural fragility and reliability of RC beams in flexure. *Structural Safety*,*26*(4), 453-470.

Stewart, M. G., & Rosowsky, D. V. (1998). Structural safety and serviceability of concrete bridges subject to corrosion. *Journal of Infrastructure systems*, *4*(4), 146-155.

Tuutti, K., “Corrosion of steel in Concrete”. Swedish Cem. And Coner.Res.Inst.,Fo4.82, Stockholm (1982).

Val, D. V., & Melchers, R. E. (1997). Reliability of deteriorating RC slab bridges. *Journal of structural engineering*, *123*(12), 1638-1644.

Vu, K. A. T., & Stewart, M. G. (2000). Structural reliability of concrete bridges including improved chloride-induced corrosion models. *Structural safety*, *22*(4), 313-333.

Zinonos,G. (2015). “Επίδραση διάβρωσης χάλυβα σε καινούριες κατασκευές οπλισμένου σκυροδέματος”, Postgraduate Thesis. Faculty of Engineering and Technology, Department of Civil Engineering and Geomatics, Cyprus University of Technology.